การศึกษาชนิดของรูปเกลือและน้ำหนักโมเลกุลของไคโตซานต่อประสิทธิภาพการนำส่ง **siRNA** เข้าสู่
เซลล์

โดย
นางสาวสิริรัตน์ วงศ์คูประเสริฐ

วิทยานิพนธ์นี้เป็นส่วนหนึ่งของการศึกษาตามหลักสูตรปริญญาเภสัชศาสตรมหาบัณฑิต
สาขาวิชาเภสัชศาสตร์ชีวภาพ
บัณฑิตวิทยาลัย มหาวิทยาลัยศิลปากร
ปีการศึกษา 2551
ลิขสิทธิ์ของบัณฑิตวิทยาลัย มหาวิทยาลัยศิลปากร

การศึกษาชนิดของรูปเกลือและน้ำหนักโมเลกุลของไคโตซานต่อประสิทธิภาพการนำส่ง siRNA เข้าสู่เซลล์

โดย
นางสาวสิริรัตน์ วงศ์คูประเสริฐ

วิทยานิพนธ์นี้เป็นส่วนหนึ่งของการศึกษาตามหลักสูตรปริญญาเภสัชศาสตรมหาบัณฑิต
สาขาวิชาเภสัชศาสตร์ชีวภาพ
บัณฑิตวิทยาลัย มหาวิทยาลัยศิลปากร
ปีการศึกษา 2551
ลิขสิทธิ์ของบัณฑิตวิทยาลัย มหาวิทยาลัยศิลปากร

THE EFFECT OF SALT FORM AND MOLECULAR WEIGHT OF CHITOSAN FOR EFFICIENCY ON siRNA DELIVERY INTO CELL

By

Sirirat Wongkupasert

A Thesis Submitted in Partial Fulfillment of the Requirements for the Degree

MASTER OF PHARMACY

Program of Biopharmaceutical Sciences

Graduate School

SILPAKORN UNIVERSITY

2008

The Graduate School, Silpakorn University accepted thesis entitled "THE EFFECT OF SALT FORM AND MOLECULAR WEIGHT OF CHITOSAN FOR EFFICIENCY ON siRNA DELIVERY INTO CELL" by Sirirat Wongkupasert in partial fulfillment of the requirements for the degree of master of pharmacy, program of Biopharmaceutical Sciences.

………………………………………..

(Assoc. Prof. Sirichai Chinatangkul, Ph.D.)

Dean of Graduate School

………./………/……..

Thesis advisors

1. Asst. Prof. Sunee   Techaarpornkul, Ph.D.

2. Assoc. Prof. Auayporn   Apirakaramwong, Ph.D.

3. Assoc. Prof. Praneet   Opanasopit, Ph.D.

Thesis committee

………………………Chairman
(Asst. Prof. Theerasak Rojanarata, Ph.D.)

……../……./…….

………………………..Member
(Asst. Prof. Sunee Techaarpornkul, Ph.D.)

……../……./…….

………………………..Member
(Assoc. Prof. Auayporn Apirakaramwong, Ph.D.)

……../……./…….

…………………………Member
(Assoc. Prof. Praneet Opanasopit, Ph.D.)

……../……./…….

…………………………Member
(Uracha Ruktanonchai, Ph.D.)

……../……./……..

49355203 : สาขาวิชาเภสัชศาสตร์ชีวภาพ
คำสำคัญ : การนำส่งเอสไอออร์เอ็นเอ / ไคโตซานรูปเกลือ / การหยุดการแสดงออกของยีน

สิริรัตน์ วงศ์คูประเสริฐ : การศึกษาชนิดของรูปเกลือและน้ำหนักโมเลกุลของไคโตซานต่อประสิทธิภาพการนำส่ง siRNA เข้าสู่เซลล์. อาจารย์ที่ปรึกษาวิทยานิพนธ์ : ภญ.ผศ.ดร.สุนีย์ เตชะอาภรณ์กุล , ภญ.รศ.ดร.อวยพร อภิรักษ์อร่ามวง และ ภญ.รศ.ดร.ปราณีต โอปณะโสภิต. 105 หน้า.

เอสไอออร์เอ็นเอเป็นอาร์เอ็นเอสายคู่ขนาดสั้นๆ มีจำนวนนิวคลีโอไทด์ 21 นิวคลีโอไทด์ ยับยั้งการแสดงออกของยีนอย่างจำเพาะเจาะจง โดยจับและเหนี่ยวนำให้เอ็มอาร์เอ็นเอเป้าหมายถูกทำลาย การทำงานนี้จะเกิดภายในเซลล์ จึงต้องอาศัยตัวพาในการนำส่งเอสไอออร์เอ็นเอเข้าสู่เซลล์ ไคโตซานเป็นพอลิเมอร์ประจุบวกชนิดหนึ่งที่เสื่อมสลายได้ภายในร่างกายและสามารถนำมาใช้เป็นตัวพาในการนำส่งเอสไอออร์เอ็นเอได้ แต่ข้อจำกัดของไคโตซานคือมีการละลายน้ำต่ำในพีเอชที่เป็นกลางและประสิทธิภาพในการนำส่งเอสไอออร์เอ็นเอเข้าสู่เซลล์เพาะเลี้ยงต่ำ เพื่อเพิ่มการละลายและประสิทธิภาพในการนำส่ง จึงใช้ไคโตซานรูปเกลือในการทดลอง การศึกษาครั้งนี้มีวัตถุประสงค์เพื่อศึกษาปัจจัยที่มีผลต่อประสิทธิภาพการยับยั้งการแสดงออกของยีน และความเป็นพิษต่อเซลล์เพาะเลี้ยง ได้แก่ ชนิดของรูปเกลือต่างๆ ของไคโตซาน (ไคโตซานไฮโดรคลอไรค์ ไคโตซานแลคเตต ไคโตซานแอสพาเตต และ ไคโตซานกลูตาเมต), น้ำหนักโมเลกุลของไคโตซาน (20, 45, 200 และ 460 kDa) และ อัตราส่วนประจุระหว่างหมู่อะมิโนของพอลิเมอร์ต่อหมู่ฟอสเฟตของเอสไอออร์เอ็นเอ (N/P ratio) เซลล์เพาะเลี้ยงที่ใช้ศึกษาการนำส่งเอสไอออร์เอ็นเอที่จำเพาะต่อยีน green fluorescence protein (GFP) คือ stable human cervical carcinoma (stable HeLa cell lines) ซึ่งสามารถสร้างโปรตีน GFP ได้ตลอดเวลา ผลการศึกษาพบว่าไคโตซานทุกรูปเกลือ และทุกน้ำหนักโมเลกุลสามารถยับยั้งการสร้างโปรตีน GFP ของเซลล์เพาะเลี้ยง ที่ระดับแตกต่างกันขึ้นอยู่กับน้ำหนักโมเลกุล พบว่าไคโตซานน้ำหนักโมเลกุลต่ำ คือ 20 และ 45 kDa มีประสิทธิภาพในการยับยั้งการแสดงออกของยีน GFP ได้สูงกว่าไคโตซานน้ำหนักโมเลกุลสูง คือ 200 และ 460 kDa พบในไคโตซานทุกรูปเกลือ ยกเว้นไคโตซานแลคเตต ที่ทุกน้ำหนักโมเลกุลให้ค่าประสิทธิภาพในการนำส่งเอสไอออร์เอ็นเอต่ำใกล้เคียงกัน และไคโตซานไฮโดรคลอไรค์ที่น้ำหนักโมเลกุล 45 kDa กับ 460 kDa ประสิทธิภาพในการนำส่งเอสไอออร์เอ็นเอให้ผลพอๆกัน เมื่อเปรียบเทียบชนิดของรูปเกลือไคโตซาน พบว่าประสิทธิภาพในการนำส่งเอสไอออร์เอ็นเอขึ้นอยู่กับอัตราส่วน N/P ratio โดยไคโตซานไฮโดรคลอไรค์ ไคโตซานแลคเตต ไคโตซานแอสพาเตต และ ไคโตซานกลูตาเมต แสดงประสิทธิภาพสูงสุด ที่อัตราส่วนดังนี้ 8 (34.2±0.5%), 16 (14.6±1.5%), 64 (32.4±4.7%) และ 64 (25.8.±1.1%) ตามลำดับ รวมทั้งมีความเป็นพิษต่อ HeLa stable cells ค่อนข้างต่ำเมื่อเปรียบเทียบกับพอลิเอทธิลีนอิมมีน

สาขาวิชาเภสัชศาสตร์ชีวภาพ   บัณฑิตวิทยาลัย มหาวิทยาลัยศิลปากร   ปีการศึกษา 2551
ลายมือชื่อนักศึกษา.......................................
ลายมือชื่ออาจารย์ที่ปรึกษาวิทยานิพนธ์ 1. .... 2. .... 3. ....

Short interfering RNA (siRNA) is a double stranded RNA (dsRNA) consisting of 21 nucleotides. siRNA inhibits gene expression specifically by binding and inducing target mRNA degradation.These mechanisms occur within a cell so vectors are important for siRNA delivery into cell. Chitosan (CS) is a biodegradable polymer with high positive charge and can be used as a vector in siRNA delivery. However the major drawback of CS is low solubility in neutral pH and low transfection efficiency. To improve the solubility and transfection efficiency, CS salt forms were used in this experiment. The purpose of this study was to investigate the effect of salt forms of CS (CS-hydrochloride (CS-H), CS-lactate (CS-L), CS-aspartate (CS-A) and CS-glutamate (CS-G)) and molecular weight (WM) of CS (20, 45, 200 and 460 kDa) and N/P ratio (charge ratio between amino groups of CS and phosphate groups of siRNA) for siRNA gene silencing efficiency and cytotoxicity. The human cervical carcinoma stable cells (HeLa stable cells), constitutively expressing green fluorescent protein (GFP) gene were used to study the delivery of siRNA targeting GFP. The results revealed that all CS salt forms were able to silence the GFP gene. The silencing efficiency depend on MW. The low MW CS (20 and 45 kDa) showed higher gene silencing efficiency than the high MW (200 and 460 kDa), observed in CS-H, CS-A and CS-G with an exception of CS-L which had low gene silencing efficiency in all MW and CS-H MW 45 show comparable efficiency to CS-H MW 460. In comparison to CS salt forms, the maximum gene silencing efficiency was found in different N/P ratios. CS-H/siRNA, CS-L/siRNA, CS-A/siRNA and CS-G/siRNA complexes showed maximum gene silencing efficiencies at N/P ratios of 8 (34.2±0.5%), 16 (14.6±1.5%), 64 (32.4±4.7%) and 64 (25.8±1.1%), respectively. Cytotoxicity results showed that all CS/siRNA complexes had cytotoxicity lower than polyethylenimine (PEI, 25 kDa).

ACKNOWLEDGEMENTS

CONTENTS

LIST OF TABLES

LIST OF FIGURES

LIST OF FIGURES

LIST OF FIGURES

LIST OF ABBREVIATIONS

AFM	atomic force microscopy
AVG	average
cm^2	square centimeter
CS	chitosan base
DD	degree of deacetylation
DNA	deoxyribonucleic acid
DMSO	dimethysulfoxide
EDTA	ethylene diamine tetraacetate sodium
e.g.	example given, for example
et al.	and others
FBS	fetal bovine serum
g	gram
GlcN	β-(1$\rightarrow$4)-2-amino-2-deoxy-*D*-glucopyranose
GlcNAc	β-(1$\rightarrow$4)-2-acetamido-2-deoxy-*D*-glucopyranose
H	hour
IC_{50}	the concentration produced 50% inhibition of the dehydrogenase activity
kDa	kilo-Daltons
L	litre
M	molar
min	minute
Mol	mole, 6×10^{23} particles

LIST OF ABBREVIATIONS

MTT	3-(4,5-dimethythiazol-2-yl)-2,5-diphenyl-Tetrazolium bromide
MW	molecular weight
N/P ratio	ratio of positively charged chitosan to negatively charged siRNA
nm	nanometer
PBS	phosphate-buffered saline
pK_a	coefficient for the acidity of a substance
pH	potentia hydrogenii (lat.)
RNA	ribonucleic acid
siRNA	short interfering ribonucleic acid
shRNA	short hairpin ribonucleic acid
SD	standard deviation
TC	tissue culture
UV	ultraviolet (spectrometry)
w/v	weight by volume
%RH	percent relative humidity
°C	degree(s) Celsius
>	more than
<	less than
µg	microgram
µl	microliter
µm	micrometer

LIST OF ABBREVIATIONS

%   percent

%v/v   percent volume by volume

%w/w   percent weight by weight

CHAPTER I

INTRODUCTION

1. Statement and significance of the research problem

A short interfering RNA (siRNA) was originally identified as an intermediate in the RNA interference pathway (RNAi). siRNA consisting of 21-23 nucleotides can regulate gene expression in mammalian cells through RNAi. (Fire et al. 1998 : 806-811; Hannon 2000 : 244-251) siRNA guides sequence-specific degradation of the homologous mRNA, thus producing "knock-down" gene. Because of the high knockdown efficiency and specificity, it has been employed as a powerful tool for curing disease by blocking the expression of a defective gene or a viral gene including cancer, viral infections and autoimmune disorders. siRNA shows many advantages over oligonucleotide antisense in terms of higher resistance to nuclease degradation and longer therapeutic effect. However, siRNA suffers particular problems including poor cellular uptake, rapid degradation by ubiquitous nucleases in blood circulation.

Basically, there are two main types of vectors that are used in siRNA delivery based on viral or non-viral vector. The viral vector shows a high transfection yield but it has many disadvantages such as oncogenic effect and immunogenicity. (Mansouri et al. 2004 : 1-8) Therefore, non-viral vector has been more attractive, as they are simple to prepare, rather stable, easy to modify and relatively safe, compared to viral vectors. Unfortunately, they also suffer from low transfection efficiency. Polycation such as chitosan, polyethylenimine (PEI), dendrimers, etc. and cationic liposomes are non- viral vectors that are widely used to deliver nucleic acids, including plasmid

DNA, antisense oligonucleotide and the more recently siRNA. (Sung and Chong 2007 : 3360-3368)

Chitosan is a copolymer of N-acetyl-glucosamine and glucosamine. This polymer is a weak base with a pK_a value of the glucosamine residue of ~6.2 to 7.0. Therefore, it is insoluble at neutral and alkaline pH values including pH 7.2-7.4 of body. To improve its solubility, chitosan is made salts form with inorganic and organic acid such as hydrochloric acid, lactic acid, glutamic acid and aspartic acid which allows it to be soluble in water. The properties of chitosan (e.g. pKa and solubility) can be modified by changing the degree of deacetylation (DD). Chitosan is a good candidate for gene delivery due to its low toxicity, biodegradability and low immunogenicity. At acidic pH, below pK_a, the primary amines in the chitosan backbone become positively charged. These protonated amines enable chitosan to bind to negatively charged DNA or siRNA and condense it into complexes.

Few researches using chitosan or chitosan salt as siRNA carriers have been done successfully. The effects of molecular weight (MW) and DD of chitosan and the N/P ratio (ratio of positive charged chitosan to negatively charged siRNA) on the complex physicochemical properties and their transfection efficiency were studied. However, the effect of salt form of CS has not been investigated. In this study we compared different CS salt including chitosan hydrochloride (CS-H), chitosan lactate (CS-L), chitosan aspartate (CS-A) and chitosan glutamate (CS-G) for their ability to form complexes with siRNA and their gene silencing efficiencies in HeLa cells, stably expressing green fluorescent protein (EGFP). Particle size and zeta potential of CS/siRNA complexes were evaluated. In addition, the cytotoxicity of CS/siRNA complexes formulated with various CS was investigated in the stable HeLa cells.

2. Objective of this research

2.1   To study the factor affecting the gene silencing efficiencies of CS/siRNA such as the salt form and molecular weight (MW) of CS and the N/P ratio.

2.2   To study the physicochemical properties of CS/siRNA complexes such as particle size, zeta-potential and morphology.

2.3   To study the cytotoxicity of CS/siRNA complexes formulated with various CS in HeLa cell.

3. The research hypothesis

3.1   Different CS salts significantly influence on the gene silencing efficiencies.

3.2   Different molecular weight of CS significantly influence on the gene silencing efficiencies.

3.3   Different N/P ratio of CS/siRNA complexes significantly influence on gene silencing efficiencies.

CHAPTER II

LITERATURE REVIEW

1. Membrane transport

The plasma membranes are a phospholipids bilayer (Figure 1). The hydrophobic lipid tails are oriented inwards and the hydrophilic phosphate groups are aligned toward the aqueous cytosol or the outside environment. The plasma membrane serves as a semi-porous barrier. It is permeable to specific molecules and allows nutrients and other essential elements to enter the cell and waste materials to leave the cell as summarized in Figure 2. The hydrophobic interior of the lipid bilayer creates a barrier to passage of most hydrophilic molecules, including ions. Electrically-neutral and small molecules such as oxygen, carbon dioxide, and water are able to pass freely across the membrane but the passage of charge and large molecules, such as amino acids and sugars are carefully regulated.

Cell is able to internalize large particles such as protein and nucleotide from the outside by adsorptive endocytosis. Endocytosis is a process where cells absorb material from the outside by engulfing it with their cell membrane which, occur first buds inward and then pinches off to form an vesicle that is called "early endosome" then, the early-endosome fuse with lysosome, resulting in the formation of "late endosome", in which the pH of late endosomes has acidified condition. Subsequently the material is digested and released into cytosol. The adsorptive endocytosis is commonly divided into two types; phagocytosis and pinocytosis. Phagocytosis, as cell-eating, involves the ingestion of large particles, such as microorganisms and cell

debris via large vesicles called phagosomes (generally >250 nm in diameter). Pinocytosis, as cell-drinking, involves the ingestion of fluid and molecules via small vesicles (<150 nm in diameter).
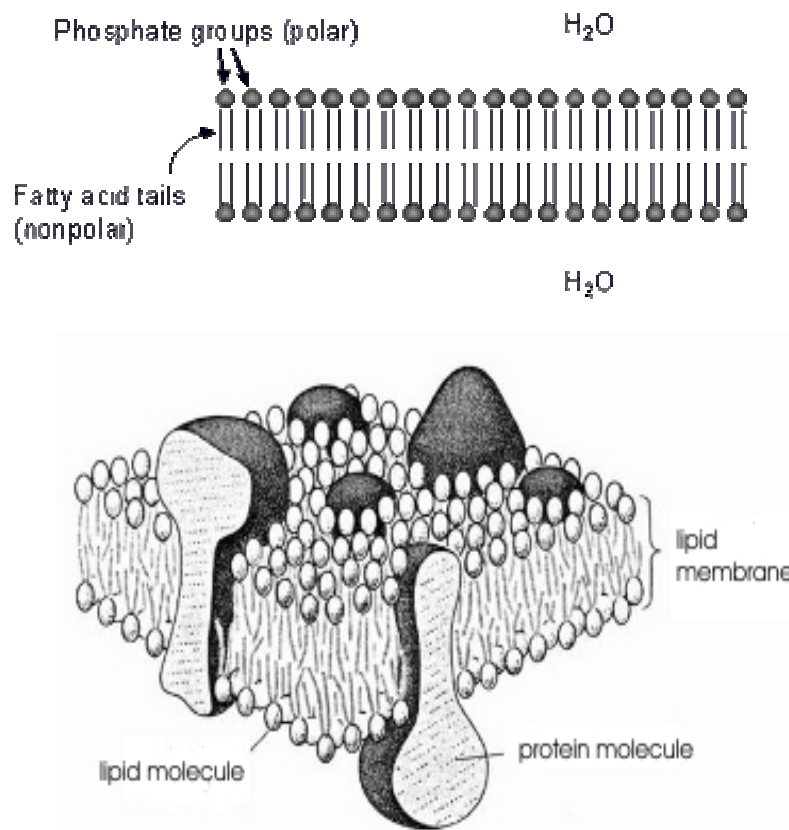
Figure 1 Schematic drawings showing the two and three-dimensional view of a cell membrane.

Source: Alberts et al, Molecular Biology of the Cell, Third edition (N.Y.: Garland Publishing, 1994), 477.

Another cell endocytosis occurs by the inward budding of plasma membrane vesicles containing proteins with receptor sites specific to the molecules being internalized that is called receptor-mediated endocytosis in which clathrin and cargo molecules are assembled into clathrin-coated pits on the plasma membrane together

with an adapter complexes called AP-2. Subsequently mature clathrin-coated vesicles

are actively uncoated and transported to early endosome (Figure 3).

Passive transport
  simple diffusion, facilitated diffusion

Small molecules

Active transport
  pumps, cootransporters

Membrane transport

Large molecules

Endocytosis
  phagocytosis, pinocytosis

Receptor-mediated

endocytosis

  clathrin-mediated endocytosis
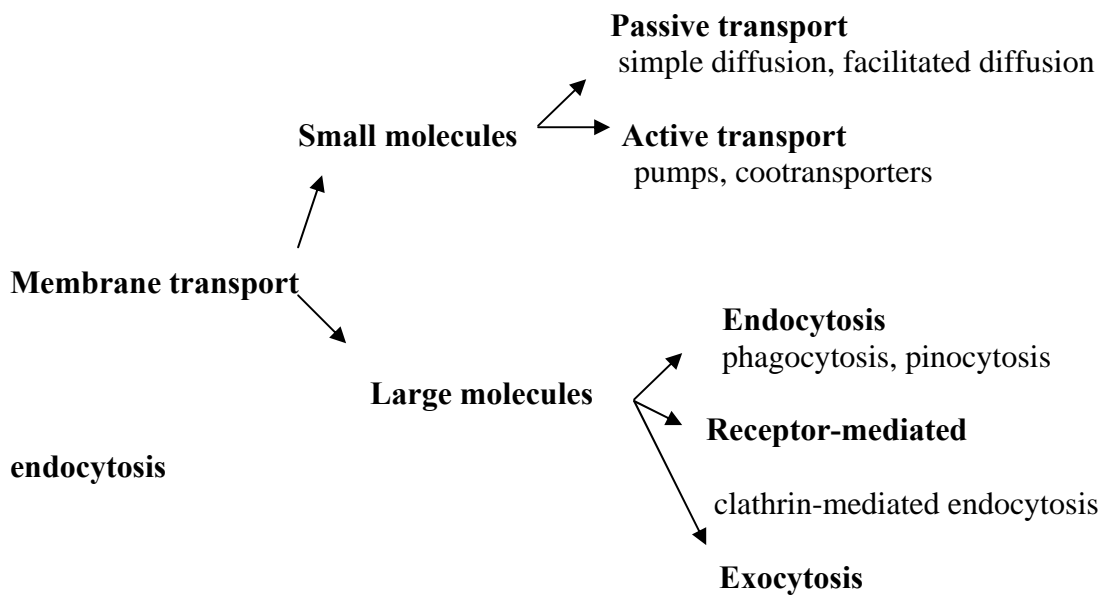
Exocytosis

Figure 2 Summary of membrane transport.
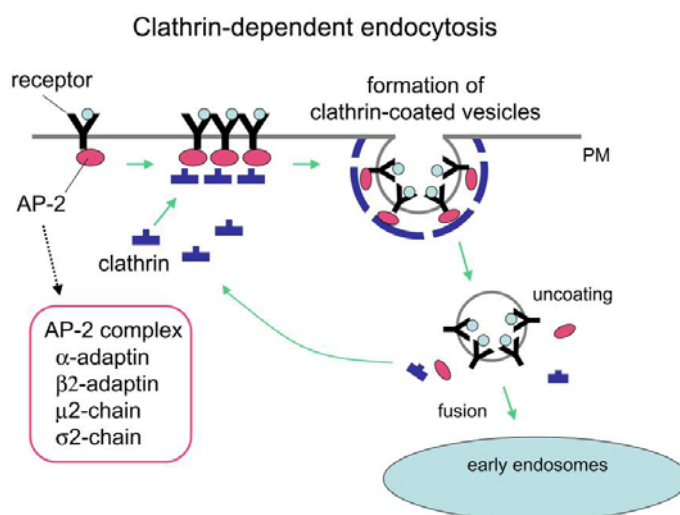
Figure 3 Mechanism of clathrin-mediated endocytosis.

Soure : Barth D. Grant, Intracellulartrafficking [online], accessed 9 May 2008.

Available from http://www.wormbook.org/chapters/www_intracellulartrafficking/txt

A number of factors influence on the cellular uptake via endocytosis including particle size, shape and surface charge. It has been reported that particles in the nanometer size have a relatively higher intracellular uptake compared to microparticles. (Zauner et al. 2001 : 39-51) Moreover, the surface charges of particles are also very important because positively charged particles interact with the cell surface by an electrostatic interaction with anionic substances on the cell surface. Negatively charged nanoparticles showed an inferior rate of endocytosis and do not utilize the clathrin-mediated endocytosis pathway. Whereas positively charged nanoparticles internalized rapidly via the clathrin-mediated pathway. (Harush-Frenkle et al. 2007 : 26-32) Therefore, gene therapy and drug delivery in nanosize particles with positive charge are considered attractive owing to their minor toxic effect and their ability to associate and internalize into mammalian cells.

2. Transfection

Transfection is a delivery of foreign genes such as DNA (deoxyribonucleic acid), RNA (ribonucleic acid) and siRNA (small interfering RNA) into eukaryotic cells. Popularly, lipofectamine 2000^{TM} (Invitrogen, USA) has been deliver siRNA into mammalian cells. Transfection has becomes a powerful tool for the study of siRNA delivery.

For successful transfection it is essential to maintain aseptic technique when working with cell cultures. The presence of microorganisms can inhibit growth, kill cells, and lead to inconsistent results. The routes of contamination are numerous such as media and reagents, instruments and pipettes, incubators and refrigerators, the worker, the hood, and incoming cells etc. Bacteria, yeasts, fungi, molds, and

mycoplasmas are common contaminants in tissue culture. Use healthy cells at optimal density. Cells should be 70–80% confluent and be used at a passage number that is well characterized. Handing of cell culture in a suitable condition is necessary for good transfection. Several stressful conditions injure cells and cause low transfection efficiency. These include frequent temperature and pH changes, inadequate nutrition from medium depletion in overgrown cultures, instability from subculturing at too low cell density, extended exposure to trypsin, exposure to shear forces from vigorous pipetting or centrifugation, and mycoplasma contamination.

3. siRNA and RNAi

3.1   History of RNAi

RNA interference (RNAi) is a post-transcriptional regulation that specifically inhibits gene expression. RNAi is generally found in all eukaryotic cells including plants and animals. RNAi has proven to be important for cellular defense against foreign genetic element such as viral genes and transposons. RNAi was first reported in 1998 by Mello and Fire et al. They found a potent gene silencing effect after injecting double stranded RNA into *Caenorhabditis elegans* (*C. elegans*) to investigate the regulation of muscle protein production, they observed that neither antisense nor sense RNA injections had an effect on protein production, but it was double-stranded RNA that successfully silenced the targeted gene. As a result of this work, they coined the term RNAi. (Fire et al. 1998 : 806-811; Hannon 2000 : 244-251)

3.2   Mechanism of RNAi

RNAi initiates when the host cell encounters a long dsRNA from a virus or an endogenous source. These long dsRNA are cleaved by dicer which is a ribonuclease III enzyme, into shorter dsRNA of 21-23 nt containing 5′ phosphate and 3′ hydroxyl termini of both strands, with 2-nt overhang at both 3′end (Figure 4). siRNA is incorporated into a nuclease complex called RNA-induced silencing complex (RISC). One of the siRNA strand, an antisense strand remaining on the RISC complex binds to the homologous nucleotide sequences within the target mRNA and induces cleavage of the mRNA, thereby preventing its translation into protein. The sense strand is removed and degraded by a helicase associated with the RISC. (Aigner 2006 : 12-25) (Figure 5).

siRNA can be exogenously introduced into cells by various form including a long dsRNA or a plasmid containing a pol III promoter that drives expression of siRNA. In mammalian cell, introduction of long dsRNA (>30 nucleotides) activated the interferon, a RNA-binding protein kinase, which induces non-specific degradation of RNA causing cell apoptosis. (Gil et al. 2000 : 107-114) Elbashir et al. succeeded in inducing RNAi machinery in mammalian cells without a non-specific response by transfecting siRNA directly into cell. (Elbashir 2001 : 494-498)

Figure 4 Schematic representation of a siRNA molecule, OH: 3′ hydroxyl.
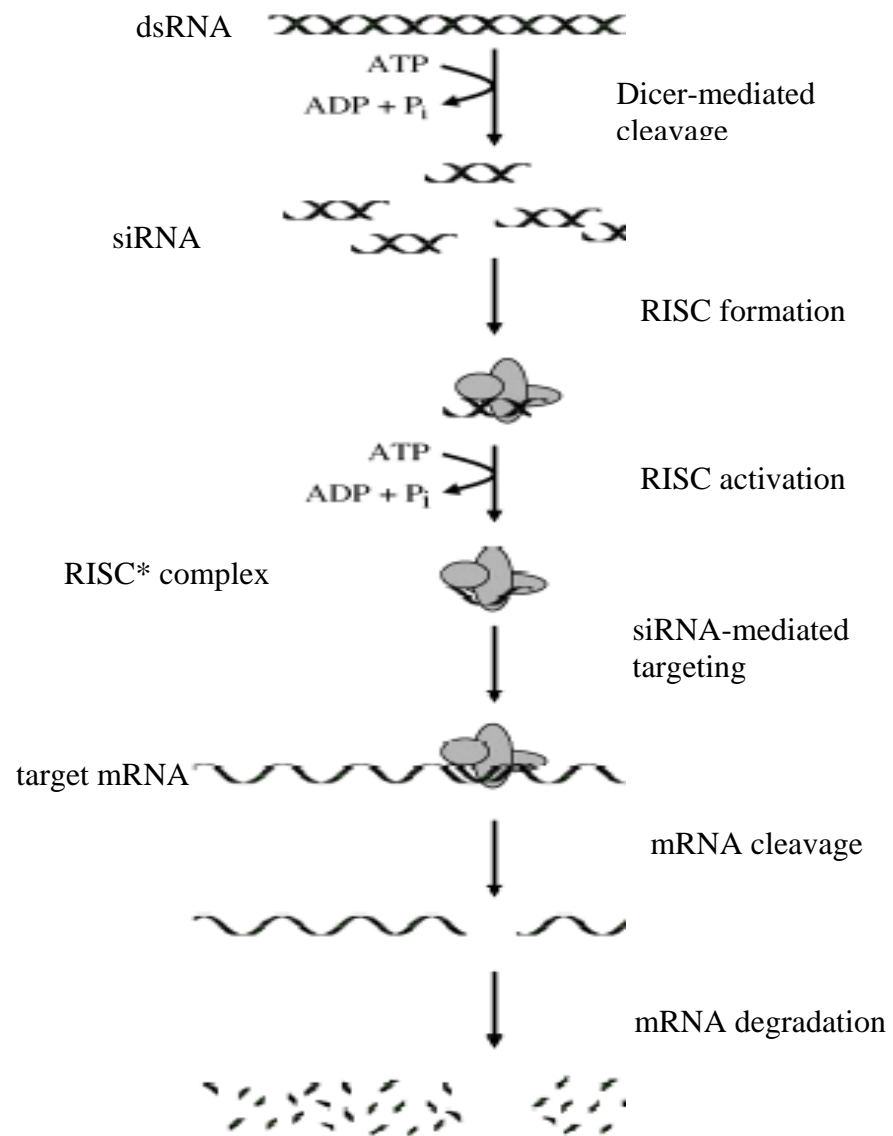
Figure 5 Mechanism of siRNA for specific gene silencing

Source : Achim Aigner, "Gene silencing through RNA interference (RNAi) in vivo:Strategies based on the direct application of siRNAs," Journal of Biotechology 124 (2006) : 14.

3.3 Application of siRNA

Any gene of which sequence is known can be targeted based on sequence complementarity with an appropriate siRNA. This has made siRNA a powerful tool for gene therapy, analyzing gene function and drug target validation. siRNA targets to viral gene or a defective gene that causes diseases has been employed for gene therapy for chronic diseases including viral infection, cancer and autoimmune disorder. At present, there are no marketed siRNA drugs but a number of siRNAs are investigated in clinical trials such as siRNA-based treatment for age-related macular degeneration is going to clinical trial at level three (Sirna therapeutics, Inc.,).

For gene function study, the expression of a targeted gene can be knocked down by siRNA and the phenotypic change can be observed as compared to the normal cell. This technique provides much simple and rapid method for the loss-of-function study compared with the conventional knockout animal technique.

3.4 Introduction of an exogenous siRNA into cell

3.4.1 Preparation of artificial siRNA

Three methods for producing synthetic siRNA are including chemical synthesis, *in vitro* transcription and siRNA expression vector. Firstly, chemical synthesis allow obtainable high purity siRNA but expensive and it is not useful for long term study. Secondly *in vitro* transcription using synthetic DNA oligonucleotide as templates. It is less expensive than the synthesis one but requires more hands-on time, high variability in yield and quality of the products. Finally, siRNA can be expressed in form of shRNA inside the cells by transfecting plasmids that consist of sequence encoding a short hairpin RNA (shRNA) under the control of an RNA polymerase III promoter. shRNA is cleaved by the cellular nuclease into siRNA. This

system provides long term target gene knock down but effective concentration of the shRNA can not be controlled.

To introduce siRNA into cell. It is advised to use high quality siRNA at the lowest effective concentration. siRNA should be free of reagents carried over from synthesis (e.g., ethanol, salts, and proteins). Double-stranded RNA contaminants longer than 30 bp can alter gene expression by activating the nonspecific interferon response, resulting in cytotoxicity.

3.4.2 Obstacle for siRNA delivery

In order for siRNA to work inside cells, they must be internalized into individual cell and access the target mRNA so the delivery of siRNA into cells, tissues or organs remain to be a big obstacle for its applications due to biophysical characteristics that frustrating the intracellular delivery of siRNA are that it is polyanionic, usually one phosphate group per residue, and macromolecular. The polyanionic character of siRNA may limit its interaction with the cell membrane to internalization via adsorptive endocytosis in regions of the cell membrane which are negatively charged under physiological condition. Consequently, the macromolecular nature of siRNA restricts its passive diffusion through the cell membrane. Furthermore, In cytosol has ubiquitous nucleases that occurring rapid degradation. Therefore, siRNA must be enclosed in carriers to allow cellular uptake, to protect siRNA from nuclease digestion and to escape endosome and release of siRNA into the cytosol where the RNAi occurs.

3.4.3 Vector used for siRNA delivery

Basically, there are two main types of vectors that are used in siRNA delivery based on viral or non-viral vector. The viral vectors show a high transfection

yield but they have many disadvantages such as oncogenic effect and immunogenicity. Therefore, non-viral vectors have attracted great interest, as they are simple to prepare, rather stable, easy to modify and relatively safe, compared to viral vectors.

Among the nonviral vector, cationic polymer and lipid-based siRNA vectors have been shown to enter cells and mediate specific RNA interference in vitro and in vivo. Cationic liposomes including lipofectamine2000 and DOPA provides high efficient siRNA transport although showing some cytotoxicity. Two cationic polymers including the natural polymers such as chitosan and its derivatives and the synthetic polymers eg. poly-L-lysine (PLL), polyethyleneimine (PEI) and dendrimers also has been used for siRNA delivery. Although they do not give as high efficiency as the cationic liposomes, in general they show lower cellular toxicity.

4. Transfection of siRNA using viral vector

There are 5 main classes of viruses used in the delivery of nucleotides to cells, including the retrovirus, lentivirus, adenovirus, baculovirus, and adeno-associated-virus (AAV). RNAi induced by viral delivery was demonstrated first using retroviral vectors based on the mouse stem cell virus (MSCV) and the moloney murine leukemia virus (MoMLV). (Brummelkamp et al. 2002 : 243-247) Despite the relative ease of use *in vitro*, use of the retrovirus *in vivo* has safety concerns and significant limitations. Retroviruses integrate their DNA into the hosts genomic DNA, bringing with it, the risk of mutagenesis and carcinogenesis. Another problem is that retroviral transduction is limited to actively dividing cells, which means that the majority of mammalian cells will not receive the siRNA. Lentiviral vectors are a promising

subclass of retroviruses that lack the risk of insertional mutagenesis and are able to transduce primary and non-dividing cells. Several studies have demonstrated the use of lentiviral vectors to deliver RNAi to target cells. Lentiviral vectors that contain Pol III siRNA-expression cassettes have been used to transfect a number of cell lines *in vitro*, including HeLa, HEK293, mouse embryonic fibroblasts, primary T cells and hematopoietic stem cells. (Stewart et al. 2003 : 493-501) Because retroviruses such as MOMLV and lentivirus integrate into the host genome, they can be used to generate stable knockdown cell lines with relatively high efficiency. At third, Adenoviral vectors are commonly used in gene therapy trials. Since the adenovirus does not integrate DNA into the hosts genome, the effects are short-lived, usually lost after several cell divisions. For this reason, the adenovirus is used when a short duration of action is sufficient or desirable, such as tumor-targeting therapy. The lack of genomic integration also provides a clear safety advantage to adenoviral vectors. Despite the lowered risk of insertional mutagenesis, the adenovirus is associated with significant dose-dependent liver toxicity that can severely limit therapy. Another major disadvantage of adenoviral vectors is the dependence on specific surface receptors on the target cell which are often absent, rendering transduction impossible in many case. Several studies have reported success in delivering siRNA to cells with an adenoviral vector using local injection. At forth, Baculoviruses are insect viruses that can carry large quantities of genetic information. This may allow their use for combined RNAi therapy and gene therapy. Safety concerns are less prominent with these vectors since the virus is unable to replicate or express proteins in mammalian cells. The last, Adeno-associated viruses (AAV) are another possible vector for siRNA. These viruses do not appear to be pathogenic and can transducer non-dividing cells. Raghvis

et al. demonstrated the ability of the modified AVV vector to delivery efficiently siRNA into HeLa S3 cells and down regulate p53 and caspase 8 expression. (Raghuvis et al. 2003 : 5712-5715)

5. Transfection of siRNA using non-viral vector

The use of viral vectors, such as retrovirus and adenovirus, to delivery siRNA has shown effective gene silencing *in vitro* and *in vivo*. (Barton 2002 : 14943-14945) Although the viral vectors show a high transfection yield but it has many disadvantages such as oncogenic effect and immunogenicity. Therefore, non-viral vectors have attracted great interest more in comparison to viral vectors due to the advantages of non-viral vectors such as simple to prepare, rather stable, easy to modify, low immune response and unrestricted gene materials size in addition to potential benefits in terms of safety. Really, siRNA is a nucleic acid, the basic principles that underlie the design of transfection reagents to delivery siRNA are similar to those used to design delivery agents for other nucleic acid, most notably plasmid DNA. Nucleic acid transfection reagents have two basic properties. First, they must interact in some manner with the nucleic acid cargo. Most often this involves electrostatic forces, which allow the formation of nucleic acid complexes. Formation of complexes ensures that the nucleic acid and transfection reagent are presented simultaneously to the cell membrane. Complexes can be divided into three classes, based on the nature of the delivery reagent : lipoplexes; polyplexes and lipopolyplexes. Lipoplexes are formed by the interaction of anionic nucleic acids with cationic lipids, polyplexes by interaction with cationic polymers, and lipopolyplexes by interaction with both cationic lipids and cationic polymers. (Felgner et al. 1997 :

511-512) Cationic lipids and cationic polymers such as chitosan, polyethylenimine (PEI) and dendrimers are non- viral vectors that are widely used to deliver nucleic acids, including DNA, antisense oligonucleotides, and ribozymes, therefore widely believed to be useful siRNA delivery reagents since siRNA, like other material genetics specially ribozymes, has negatively charged phosphate groups that allow electrostatic complexation. Furthermore, size of siRNA, near ribozymes, consist short chain of ribonucleotide sequence.

5.1 Cationic liposomes (Lipoplexes)

Many cationic liposomes/lipid-based products are commercially available, including lipofectamine2000, N-[1-(2,3-Dioleoyloxy) propyl]-N ,N ,Ntrimethylammonium methylsulfate (DOTAP) and N-[1-(2,3-dioleyloxy) propyl]-N,N,N-trimethylammonium chloride (DOTMA). As early as the late 1980s, DOTMA was the first liposome that was used to transfer DNA and RNA. (Malone 1989 : 6077-6081) Lipofectamine2000 is a cationic liposome based reagent that provides high transfection efficiency for both DNA and siRNA in a range of mammalian cell types *in vitro*. Lipofectamine2000 has also been used successfully to transfect synthetic siRNA into mammalian cells for RNAi studies. Dalby et al. used lipofectamine2000 to investigate the effect of these factors on its transfection efficiency to siRNA. (Dalby 2004 : 95-103) Khoury et al. demonstrated cationic lipid 2-(3-[bis-(3-amino-propyl)-amino]-propylamino)-*N*-ditetradecylcarbamoylme-thyl-acetamide combined with L-alpha-Dioleoyl Phosphatidylethanolamine (DOPE) can be efficient to deliver siRNAs designed to silence tumor necrosis factor α (TNF-α) in collagen-induced arthritis (CIA). (Khoury 2006 : 1867-1877)

5.2 Cationic polymers (Polyplexes)

5.2.1 Polyethylenimine (PEI)

Polyethylenimine (PEI) is a polymer with high positive charge density of amine groups. It can form electrostatically complex with the negatively charged phosphate groups of nucleic acid to produce a neutral or positively charged complex to allow intracellular delivery of the genetic material. PEI is also believed to facilitate nucleic acid delivery through a proton sponge mechanism wherein the osmotic pressure at acidic pH is enhanced causing rupture and release of nucleic acid within endosomal vesicle. (Akinc et al. 2005 : 657-663) PEI exists in two principal forms, branched (25 and 800 kDa) and linear (25 kDa) (Figure 6), have been successfully used as transfection agents. Recently, application of linear PEI or low molecular PEI as an siRNA delivery vector has been becoming a hot research subject. Grayson et al. evaluated the efficacy of different PEI structures for siRNA delivery in the HR5-CL11 cell line stably expressing luciferase. Only 25 K B-PEI was found to successfully mediate siRNA delivery and occurred only when an N/P ratio of 6:1 or 8:1 was used with an siRNA concentration of 200 nM. The zeta potential and size of the complexes correlated to transfection efficacy for complexes formed from the 25 K B-PEI and 800 B-PEI, but not the 22 K L-PEI. Other factor, such as the relative stability of the complexes, may also play a role in determining the transfection efficacy of a given PEI structure. The ability of PEI to transfer siRNA into cells is surprisingly dependent on its biophysical and structure characteristics when compared to its relative simple for DNA delivery. Therefore, siRNA transfection is apparently different from DNA transfection. (Grayson et al. 2006 : 1868-1876) Werth et al. showed that PEI F25-LMW (PEI 25 K, low molecular weight, fresh complexes) was

able to complex and fully protected siRNA against nucleolytic degradation, and delivered siRNAs into PC-3 cells (prostate carcinoma cells) where they displayed bioactivity. Upon lyophilization and reconstitution of the complexes, siRNAs were still able to efficiently induce RNAi. (Werth et al. 2006 : 257-270)

5.2.2 Dendrimers

Polycationic dendrimers such as poly (amidoamine) (PAMAM) dendrimers are known to be efficient nucleic acid delivery system. These dendrimers bear primary amine groups on their surface, while having tertiary amine groups inside. The primary amine groups participate in DNA binding, compact DNA into nanoscale particles and promote the cellular uptake of DNA, while the buried tertiary amine groups act as a proton sponge in endosomes and enhance the release of DNA into the cytoplasm. All these features of dendrimers could also be used for RNA delivery. Zhou et al reported that PAMAM dendrimers show strong binding affinity for RNA molecules. They developed dendrimers with the triethanolamine as core has the branching unit starting 10 successive bonds from the center amine (Figure 7). Dendrimers used in this study are referred as G_n (n: dendrimer generation number). The first studied the ability of dendrimers to from self-assembled complexes with siRNA by performing agarose gel electrophoresis. Dendrimers with amine end groups were able to almost completely retard siRNA in the gels at N/P ratios > 2.5. Moreover, the ability of siRNA/dendrimer complexes to deliver siRNA to A549Luc cells stably expressing the GL3 luciferase gene was tested using a model of endogenous gene knockdown. Efficient gene silencing was observed with the specific GL3Luc siRNA-G_7 complexes, while neither the naked siRNA nor the nonspecific GL2Luc siRNA-G_7 complex showed any gene silencing effect. These results are a

consequence of efficient dendrimers-mediated siRNA delivery. The conclusion, the effective siRNA delivery system based on structure flexible polycationic PAMAM dendrimers. These genuine, nondegraded dendrimers condense siRNA into nanoparticles. They protect siRNA from enzymatic degradation and achieve substantial release of siRNA over an extended period of time for efficient gene silencing. Taken together, these findings suggest that flexible polycationic dendrimers may have great potential for *in vitro* (functional genomics) and possibly *in vivo* (therapeutic) applications. (Zhou et al. 2006 : 2362-2364)
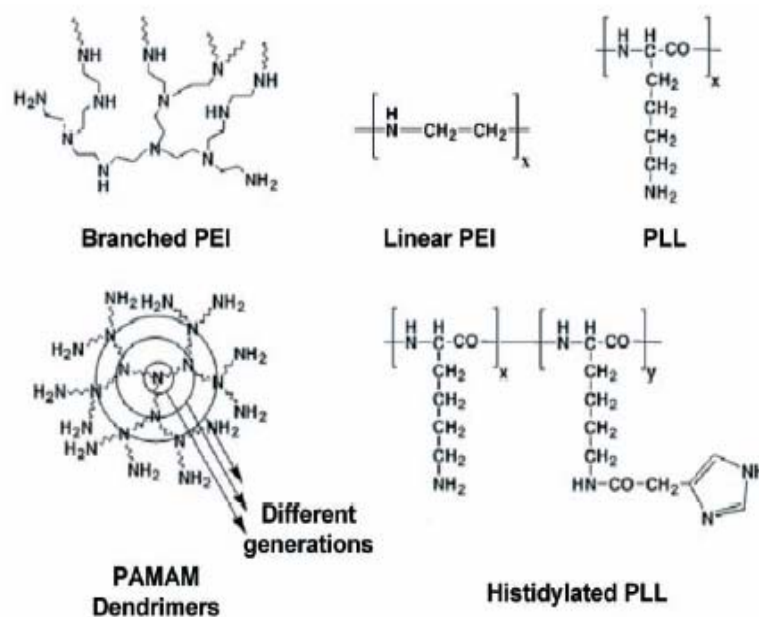
Figure 6 Cationic polymer most commonly used for nucleic acid delivery

Souce : Thomas Merdan et al., "Prospects for cationic polymers in gene and oligonucleotide therapy against cancer," Adv Drug Deliv Rev 54 (2002) : 58.
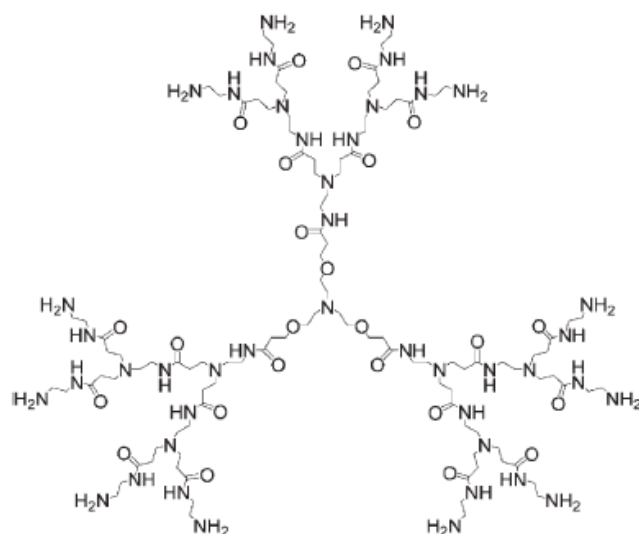
Figure 7 Chemical structure of PAMAM dendrimers with triethanol-amine as core

Souce : Jiehua Zhou et al., "PAMAM dendrimers for efficient siRNA delivery and potent gene silencing," <u>Chem communication</u> 4 (2006) : 2362-2364.

6. Chitosan

Chitosan (CS), a (1→4) 2-amino-2-deoxy-β-D-glucan, is a linear cationic aminopolysaccharide derived by partial alkaline deacetylation of chitin Figure 8. (Skaugrud 1989 : 31-35), a polymer abundant in nature. Chitin is mostly obtained from exoskeletons of crustacean; main sources are shell wastes of shrimp and crab. Chitin also exists naturally in some microorganisms and fungi such as yeast. The backbone of the copolymer consists of two subunits, D-glucosamine and *N*-acetyl-D-glucosamine, which are linked by 1→4 glycosidic bonds. The process of deacetylation involves the removal of acetyl groups from the molecular chain of chitin, leaving behind a compound (chitosan) with a high degree chemical reactive amino group (-NH$_2$). Molecular weight of native chitin is usually larger than one million Daltons (Da) while commercial chitosan products have the molecular weight

range of 10,000-1,000,000 Daltons, depending on the process and grades of the product. These two characteristics are important because of their heavy impact on the physicochemical, biological and the formulation properties of chitosan.

6.1 Properties of chitosan

Chitosan is weak base with a pKa value of approximately 6.2-7.0 on the amino groups; it is insoluble at neutral and alkaline pH values. However, it can form water-soluble salts with acids such as hydrochloric, lactic, glutamic and aspartic acid, which products were called "chitosan salt form". Upon dissolution in acid media, the free amino groups (controlled by degree of acetylation) become protonated, resulting in a high charge density and a fully extended, flexible conformation of the chitosan backbone. (Harish Prashanth and Tharanathan 2007 : 117-131) The characteristics of glucosamine unit and acid used to form salt form was presented in Table 1.
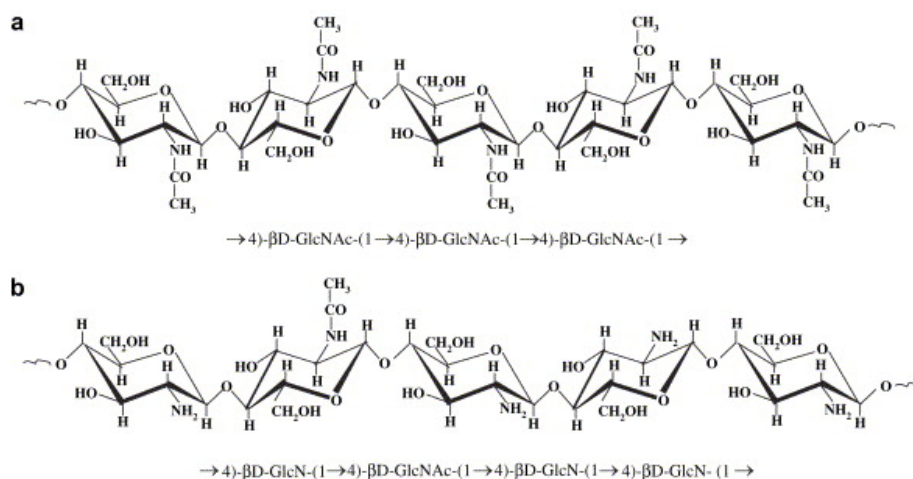
Figure 8 Primary structure of (a) chitin and (b) chitosan

Source : Harish Prashanth and Tharanathan, "Chitin/chitosan : modifications and their unlimited application potential-an overview," Trends in food science & technology 18 (2007) : 119.

The viscosity of chitosan solutions varies from low to high depending on factors such as the molecular weight (MW), degree of deacetylation, pH, ionic strength and temperature. (Wang 1994 :149-152) Protonated chitosan can form gels with polyanions, a property that was exploited in the development of controlled-release formulations of various drug.

The possibility of chemical modification of chitosan, for instance, by introducing chemical groups to its backbone structure through covalent binding has resulted in a series of versatile chitosan derivatives with improved physicochemical properties and transfection efficiency such as quaternized CS have been synthesized in order to free amine groups of CS can form ammonium salts with inorganic and organic acids. Reaction of CS with excess of methyl iodide in alkaline condition give *N*-trimethyl CS derivative. Such quaternary CS derivatives are useful for enhance solubility. (Thanou 2002 : 153-159)

Chitosans, except for high molecular weight chitosans of specific salt forms, are generally shown to be nontoxic (LD50 in rats of 16g/kg) (Borchard and Bivas-Benita, in Amiji 2004 : 301-310), partially due to their biodegradabity. Chitosan is degraded by lysozymes into a common amino sugar, which is incorporated into the synthetic pathway of glycoproteins, and is subsequently excreted as carbon dioxide.
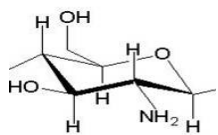
6.2 Applications of chitosan

The application potential of chitosan is abundance such as in food and nutrition, biotechnology, material science, drugs and pharmaceuticles, agriculture and environmental protection, and recently in gene therapy as well. Examples of potential applications of chitosan in conventional pharmaceutical include its use as binder, disintegrant and coating material. Because of its unique polymeric character, gel-

forming properties and property for degradation, chitosan-based controlled and targeted delivery systems have also been developed and examined. Several reports have confirmed the absorption enhancing characteristics of chitosan formulations following nasal administration of vaccines, peptides, proteins and low molecular weight drugs. (Davis et al. 2003 : 1107-1128)

In recent years, chitosan-based carriers are one of the non-viral vectors that have gained increasing interest as a safer and cost-effective delivery system for gene materials including plasmid DNA (pDNA), antisense, oligonucleotides and siRNA. At acidic pH, the primary amine functions are protonated, resulting in a cationic polymer of high charge density, which can easily form stable complexes with negatively charged nucleotides by electrostatic interaction, partially protecting genetic material from nuclease degradation.

Table 1 Characteristics of acid and glucosamine unit of chitosan salt.

Acid	M.W.	bp (°C)	mp (°C)	pK$_a$	Chemical structure
L-Aspartic	133.10			3.65	COOH HC-NH$_2$ CH$_2$ COO$^-$
L-Glutamic	147.13		160	4.25	COOH HC-NH$_2$ CH$_2$ CH$_2$ COO$^-$
Lactic	90.08	122	17	3.86	CH$_3$ HC-OH COO$^-$
Hydrochloric	36.4	110			Cl$^-$
Chitosan	161.16			6.3 – 7	

Source : Garnpimol Ritthidej et al., "Moist heat treatment on physicochemical change of chitosan salt films," International Journal of Pharmaceutics 232 (2002) : 11.

6.3 The complex formation between CS and siRNA

Katas et al. was the first group to investigate the use of chitosan to deliver siRNA *in vitro*. They used 2 MW of CS-H and CS-G to form CS/siRNA complexes by three methods; simple complexation, ionic gelation by siRNA entrapment in chitosan-tripolyphosphate (CS-TPP) nanoparticles and by adsorption of siRNA onto the surface of preformed CS-TPP nanoparticles. These complexes were evaluated for their physicochemical properties and their siRNA delivery efficiency. They found that siRNA CS-TPP entrapment in nanoparticles showed higher transfection efficiency than those prepared by the other two methods possibly due to their high binding and loading efficiency. (Katas and Alpar 2006 : 216-225) Liu et al. studied the gene silencing activity and the physicochemical properties (size, zeta potential, morphology and complexes stability) of the CS/siRNA complexes. (Liu et al. 2007 : 1280-1288) The chitosan properties that have effect on the gene silencing activity and the physicochemical properties of the particles include molecular weight (MW), degree of deacetylation (DDA) and N/P ratio.

6.3.1. The effect of MW and DD

The molecular weight and degree of deactylation of chitosan are important factors that determine siRNA compaction, the nuclease resistance of the complexes and the dissociation of siRNA from chitosan. The higher MW CS are longer and more flexible molecules whereas the lower MW CS are shorter and have stiffer molecular chains. The DD value determines the positive charge density when chitosan is dissolved in acidic conditions. Higher DD results in increased positive charge enabling a greater siRNA binding capacity.

Liu et al. investigated the effects of MW and DD of CS on physicochemical properties of CS/siRNA complexes and gene silencing efficiency. They formulated siRNA/chitosan nanopaticles at N:P 50 using different chitosan samples (MW range was 8.9-173 kDa and DDA range was 54- 95%) as shown in Table 2 .

Table 2   Chitosan samples with different MW and DD

Simple	C9-95[a]	C12-77	C65-78	C114-84	C170-84	C173-54
MW (kDa)	8.9	11.9	64.8	114.2	170	173
DD (%)	95	77	78	84	84	54
SIZE	3500	500	200	200	200	200

[a]Numbers indicate MW (molecular weight, kDa) and DD (degree of deacetylation, %).

The result showed that the size of nanoparticles formed with chitosan C9-95 (low MW and high DD) was ~3500 nm and decreased to ~500 nm with chitosan C12-77 (low MW and medium DD). All other chitosan samples (C65-78, C114-84, C170-84, and C173-54) resulted in particles with a size of approximately 200 nm. The zeta potential for all formulations was in the range of 10-20 mV, suggesting a net positive surface charge due to excess chitosan. The charge increased slightly with MW, with the exception of C173-54 which was reduced due to the relative low DD value.

Study of gel retardation assay and in vitro transfection in EGFP stably expressing human lung carcinoma cells (H1299) revealed that low MW CS ~10 kDa even with DD as high as 95% cannot form complex and show low or no gene silencing whereas the high MW CS ~64-170 kDa with medium DD (77-84%) can

form stable complex resulting in 45-65% gene silencing efficiency. The high MW CS with low DD of 54% form unstable complex with lower positive charge and lower gene silencing efficiency than those CS with higher DD. (Liu et al. 2007 : 1280-1288)

Katas et al. studied 2 chitosan salt with 86% DDA: chitosan hydrochloride and chitosan glutamate. The result showed that smaller particle size was obtained with the lower MW (CS-H 110 kDa versus CS-H 270 kDa, and CS-G 160 kDa versus CS-G 460 kDa) or the lower concentration of chitosan. They explained that due to the decreased viscosity of the lower MW and concentration of chitosan which resulted in better solubility and generated its molecular character as a polyelectrolyte material that allows more efficient interaction between negatively charged siRNA and the cationic chitosan. (Katas and Alpar 2006 : 216-225)

6.3.2   The effect of N/P ratio

The transfection efficiencies were significantly influenced by the N/P ratios, which defined as the theoretical charge ratio of chitosan amino groups (N) to siRNA phosphate groups (P). The N/P ratio can be used to control the characteristics of the formed complexes such as condensation, stability, zeta-potential, size and transfection efficiency of complexes. Liu et al. showed that the complex stability and the level of EGFP knockdown increased at higher N:P ratio formulations compared to lower N:P formulations. Nanoparticles of siRNA and high MW CS with 84% DD formed at N:P 150 showed the greatest level (~80%) of EGFP knockdown. Nevertheless, the high N/P ratio formulations show slightly increase in cytotoxicity which may be due to the increased level of free excess CS in the system. (Liu et al. 2007 : 1280-1288)

6.4 The mechanism of gene silencing via chitosan/siRNA complexes

In general, it is thought that the intracellular trafficking of siRNA occurs by endocytosis, followed by release from the endosome, and silencing messenger RNA (mRNA) that it recognizes as having the complimentary sequence. The siRNA/chitosan complexes consists of the negatively charged active siRNA sequences that are designed to "silence" target gene. These siRNA sequences are complexed through electrostatic bonds with the chitosan cationic polymer. Previously, it has been well accepted that the siRNA/chitosan complexes absorb to the cell surface through electrostatic interactions and internalized into the cells by endocytosis. Recently, there have been several evidences suggesting that chitosan interacts with cell membranes not only by electrostatic forces, but also by interactions with carbohydrate moieties on cell membranes. These interactions lead to a disturbance of the bilayer structure. (Borchard and Bivas-Benita, in Amiji 2004 : 301-310)

After the siRNA/chitosan complexes have already been internalized into cell, they must be escape from endosomal vesicle to avoid lysosomal degradation into the cytoplasm. Exactly what happens inside the endosome to release the nanoparticles is still not fully understood, even for delivery of pDNA. What is known is that following endocytosis, nanoparticles are sequestered in vesicle inside the endosome where enzymes and the acidic pH (~5.5) can either degrade or swell polymers, depending on their chemistry. This step may help to release the nucleic acid from the nanoparticles, but if the naked DNA or siRNA remain inside the endosome for too long, it will also be degraded. (Bettinger et al. 2001 : 3882-3891) Katas et al. reported that the siRNA/chitosan nanoparticle complex significantly protected siRNA from nuclease

activity. In this study siRNA/CS-TPP complex up to 72 h in 5% serum and 7 h in 50% serum whereas naked siRNA was degraded after 48 h of incubation in 5% serum and instantly degraded in 50% serum. (Katas and Alpar 2006 : 216-225)

Finally, siRNA which escapes from the late endosome, was released into the cytosol where RNA-Induced Silencing Complex (RISC) was activated. RISC encountered siRNA, unwinded it leaving only the antisense strand then bound and located to target messenger RNA (mRNA) with homologous nucleotide sequences and induced cleavage specific of mRNA.

7. Establishing a stable cell line constitutive expressing EGFP gene

Green fluorescent protein (GFP) from the bioluminescent jellyfish *Aequorea Victoria*. GFP is unique among various light-emitting proteins in being autofluorescent. i.e. it does not required substrate or cofactors to emit light. Moreover, mutants of GFP can be generated to increase fluorescence intensity and shift wavelengths of excitation and emission. A plasmid encoding enhanced green fluorescent protein (EGFP) gene was used to generate a stable cell line producing EGFP. This stable cell line can be uses as a model to test for specific eGFP gene silencing activity and the cytotoxicity of the complexes containing siRNA targeting EGFP.

The pEGFP-C2 plasmid DNA (Figure 9), Genebank accession #: U55761, encodes a red-shifted variant of wild-type GFP which has been optimized for brighter fluorescence and higher in expression in mammalian cells. (Excitation maximum = 488 nm; emission maximum = 507 nm.). The plasmid contains neomycin/kanamycin resistant gene as a selectable marker for selection of transfectants using a

commercially available G418 antibiotic. Cells that have successfully integrated the transfected pEGFP-2 into their chromosomal DNA will form clones of stable cell lines expressing EGFP gene constitutively when growing in a complete medium with G418.
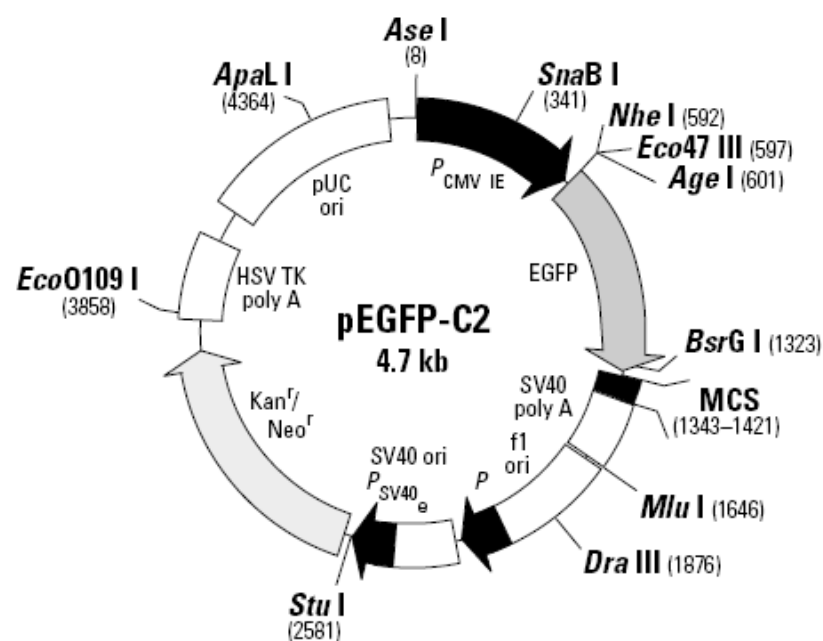
Figure 9 Schematic representation of a pEGFP-C2 vector.

Source : Clontech company, Plasmid map [online], accessed 10 May 2008. Available from http://www.clontech.org/chapters/plasmid pEGFP-C2 /txt.

CHAPTER III

MATERIALS AND METHODS

1. Materials

1.1 siRNA-EGFP(+) targeted to position 124-145 of the *eGFP* open reading frame (sense: 5' –AAG CUG ACC CUG AAG UUC AUC-3', antisense: 3' –CGA CUG GGA CUU CAA GUA GAA-5') and non-silencing control, siRNA-EGFP(-), (sense: 5' –AAG CAC CGC UUA CGU GAU ACU-3', antisense: 3' –CGU GGC GAA UGC ACU AUG AAA-5'), 5 nmol each, were purchased from Ambion, USA (Silencer® GFP (eGFP) siRNA, Catalog # : AM 4626)

1.2 Chitosan (CS) MW of 20, 45, 200 and 460 kDa with 85% degree of deacetylation (Seafresh company, Thailand)

1.3 The HeLa cell line was obtained from Nanotec Thailand (American Type Culture Collection Catalog No. CCL-2 TM) at passage number 77.

- Tissue culture reagents including Minimum Eagle Medium (MEM), Fetal bovine serum EU approved, origin L-Glutamine, MEM non-essential amino acids, trypan blue stain 0.4% and 0.25% Trypsin-EDTA were purchased from GIBCO^TM, USA

1.4 Plasmid encoding green fluorescence protein (pEGFP-C2) and materials for purification of plasmid

1.5 *Escherichia coli* DH5-α

1.6 All other chemicals

Geneticin (G418) (Invitrogen , USA)

Lipofectamine 2000^{TM} (Invitrogen, USA)

Diethylpyrocarbonate (DEPC) (Bio basic INC, Canada)

GenePure LE Agarose (ISC BioExpress®, USA)

 Sodium bicarbonate (Fisher Scientific, USA)

3-(4,5-dimethylthiazol-2-yl)-2,5-dipheny-tetrazolium bromide (MTT) (Sigma-chemical company, USA)

L (+)-Aspartic acid, 98+% (ACROS ORGANICS USA, Belgium)

L-Glutamic acid (Merch, Germany)

Lactic acid (VWR International Ltd., England)

Hydrochloric acid (Merch, Germany)

Lambda DNA / *Hin*d III Markers (Promega, USA)

Blue/Orange 6X loading dye (Promega, USA)

LB medium (Pacific Science Co., Ltd, Thailand)

2. Equipment

1. Spray dryer (Minispray Dryer, Büchi 190, Postfach, Switzerland)

2. Atomic force microscopy (SPI4000-SPA400, Seiko Instruments, Chiba, Japan)

3. Spectrophotometer (Agilent Technologies, Waldbronn, Germany)

4. Zetasizer 3000 (Malvern Instruments, Southborough, MA, USA)

5. CO_2 Incubator (Contherm, Lower Hutt, New Zealand)

6. Laminar hood (Holten, Nino-lab, Sweden)

7. Optical microscope (Nikon, eclipse TE2000-S, Tokyo, Japan)

8. Incubator shaker (GFL, Burgwedel, Germany)

9. Microplate reader (Universal Microplate Analyzer, AOPUS01 and AI53601, Packard Biosciences, Meriden, CT, USA)

10. Gel electrophoresis set (Alphaimager 2200, Alpha-Innotech, CA, USA)

11. Cell culture plate/ dish / flask (Corning, NY, USA)

12. pH meter (Horiba, Kyoto, Japan)

3. Methods

3.1 Preparation of plasmid

One hundred nanogram of plasmid pEGFP-C2 was transformed into *Escherichia co*li DH5-α (*E. Coli*), plated on LB agar supplemented with 50 μg/ml of Kanamycin (Invitrogen, USA) and incubated overnight at 37 °C. A single colony of transformant was grown in 100 ml of LB medium at 37 °C with vigorous shaking at 200 rpm. The cells were harvested by centrifugation at 6000 g for 15 minute at 4°C. The plasmid was isolated from the pellet using QIAGEN$^{\circledR}$ Plasmid Midi Kits (QIAGEN, USA), according to the manufacturer's directions. The concentration of prepared plasmid was determined by spectrophotometry (Biometra$^{\circledR}$, USA) at wavelength 260 nm and 280 nm. The concentration of plasmid was calculated using follow equation:

| Plasmid concentration | = | 50 μg/ml | x | OD_{260}nm | x | DF |

- A solution of 50 ug/ml of an average double-stranded DNA has an OD_{260} nm of 1.

- OD_{260} nm is the optical density from the absorbance reading

- DF is the dilution factor

3.2 Preparation of Chitosan salts

Chitosan base (CS) with MW of 20, 45, 200 and 460 kDa and 85% degree of deacetylation (DD) was dissolved in dilute acid solutions of hydrochloric acid, lactic acid, glutamic acid and aspartic acid in certain molar ratio (Table 3). These solutions were adjusted with distilled water to make1% w/w solutions and stirred for at least 12 h, filtered and then spray-dried at a feed rate of 5 ml/min under the following conditions: inlet temperature of 125 ± 2 ^{0}C and outlet temperature of 65 ± 2 ^{0}C using a spray dryer (Minispray Dryer, Büchi 190, Switzerland). The obtained powders (CS-H, CS-L, CS- CS-G and CS-A) were stored in a dessicator containing dry silica gel prior to use in each experiment. (Nunthanid et al. 2004: 15-26)

Table 3. Molar ratio of D-glucosamine unit : acids

Materials	Molar ratio	Chitosan salts
chitosan: aspartic acid	1:0.850	CS-A
chitosan: hydrochloric acid	1:0.800	CS-H
chitosan: glutamic acid	1:0.825	CS-G
chitosan: lactic acid	1:0.775	CS-L

3.3 Preparation of complete growth medium

The process of preparation of 1X complete culture medium is shown as follows: fetal bovine serum (FBS) was heat-inactivated by incubating for 30 min in a 56°C water bath. To prepare 1 litre of medium, MEM medium powder (GIBCO,

USA) was dissolved in 300 ml of sterile water with gentle stirring and 2.0 g of NaHCO$_3$ was added and the pH was adjusted to 7.4-7.5 using 1 M HCl or 1 M NaOH before adding more sterile water to adjust the volume to 1L. The medium was sterilized immediately by 0.22 μm membrane filtration. Then the medium was supplemented with: 1% v/v L-Glutamate, 1% v/v Non-essential amino acid and 10% v/v heat- inactivated FBS.

3.4 Establishing stable cell lines

HeLa cells were transfected with complexes of 0.8 μg of pEGFP-C2 plasmid DNA (Clontech , USA)   and 2.0 μl of lipofectamine2000^{TM} (Invitrogen, USA) according to the manufacturer's instructions. Briefly, the day before transfection, cells were seeded 1×10^5 cells into each of one well of a 24-well plate and incubated at 37 °C with 5% CO$_2$. Prior to transfection, medium was removed and washed one time with PBS then added with a mixture of 100 μl of complexes and 500 μl of serum free medium then incubated at at 37 °C with 5% CO$_2$ incubator for 12 hours then the medium was removed and was added fresh medium and further incubation until cell growed 100 % confluent. Cells were trypsinized and aliquot into a 100 mm cell culture dishes and added with selective medium, a MEM supplemented with 10% FBS and 0.5 mg/ml of G418 (Geneticin® Invitrogen Corp, USA) which is used to select and maintain for EGFP gene expression. Later, the cells were maintained in selective media to get single clone of a few hundreds cells (Figure 10-11). Media were changed every 3 days. Individual clones were isolated and transferred into each of 24-well plate and cultured in MEM supplemented with 10% FBS and 0.1 mg/ml of

G418. The cells were subpassaged and expanded in separate wells of 6-well plate. Cryostocks of each clone were collected from 100% confluent cell culture.

3.4.1 The cultivation of HeLa stable cells

HeLa stable cells were grown in 250 ml tissue culture flask containing complete growth medium (MEM) in a humidified air atmosphere (5% CO_2, 95% RH, 37 °C). Cultivated cell were visualized using an inverted microscope to detect cross-contamination or visible microbial contamination. The cells were subpassage every 3-5 days as spit ratio of 1:5 to 1 :10.
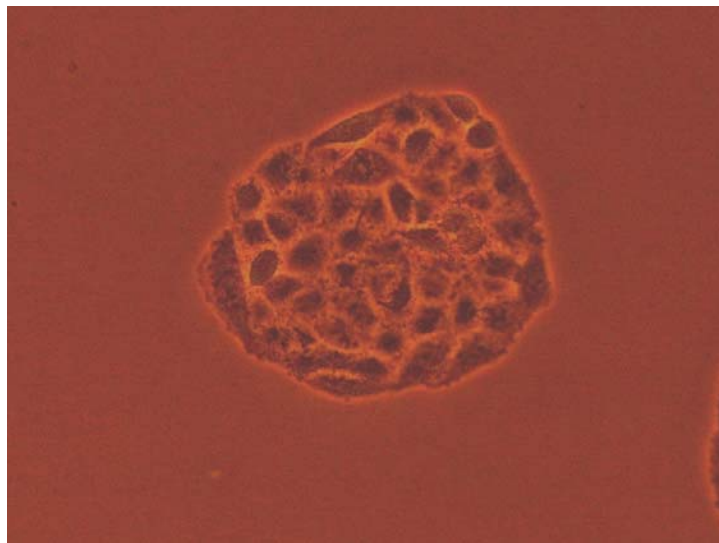
Figure 10 Cultivated HeLa cells on 24-well plate. image 10x objective using an

inverted microscope.

.
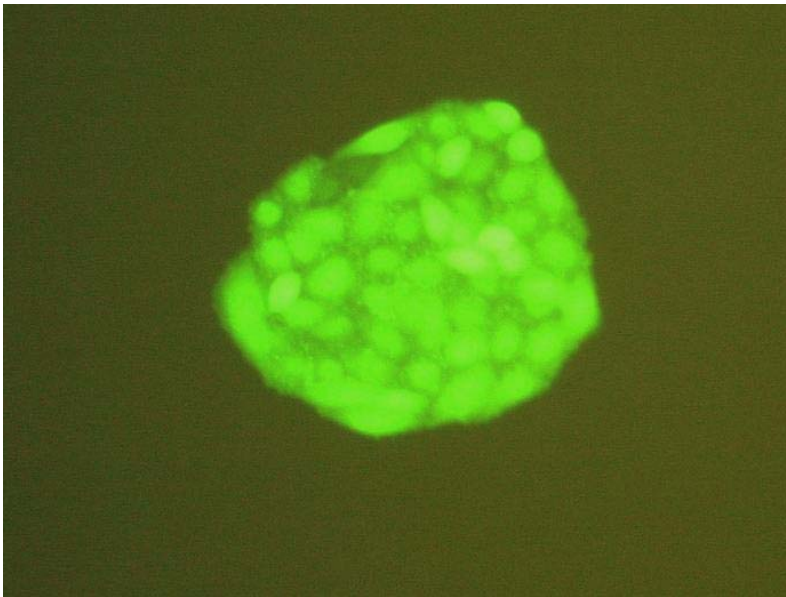
Figure 11 Cultivated HeLa stable cells on 24-well plate. image 10x objective

using fluorescent microscope.

3.4.2 Thawing frozen cell

Thaw the frozen cells in a vial by gentle agitation in a 37 °C water

bath. Thawing should be rapid and transfer the vial contents to a sterilized tube

containing 10 ml complete medium. The cells were briefly centrifuged at 1,000 rpm

for 1 min at 4 °C to remove DMSO containing medium that can be toxic to cell. The

medium was removed and the cell pellet in complete growth medium was

resuspended gently. The cell suspension was diluted to appropriate concentration, and

transferred into a tissue culture flask.

3.4.3 Subculturing

The cells were subpassaged when reaching 80-100% confluency. The

medium was aspirated and the cells were rinsed one time with PBS before adding 1

ml of 0.25% trypsin/EDTA solution (GIBCO, USA) and incubating at 37°C for approximately 5 minutes or until the cells detach and float. This can be confirmed by periodic visual inspection of flasks or observing cells under an inverted microscope. Inactivate trypsin/EDTA by adding excess serum-containing medium. Cell suspension was removed to a conical tube and pellet by centrifugation at 1,000 rpm for 1 minute. 5 ml of complete culture medium was added and the cells were resuspended gently by pipette up and down. For spit ratio 1:5, 1 ml of the cell suspension were added to a new 75 cm^2 TC flask and 15 ml of complete culture medium was added. The cell culture was then placed in the incubator.

3.4.4 Frozen culture

For one 75 cm^2 cell culture flask, cells were trypsinized, pelleted and resuspended in 5 ml of complete culture medium. The cell suspension tube and 5 labeled cryotubes were pre-cooled on ice for 5 minutes before adding 250 μl of DMSO into the suspension cell and mixing gently. 1 ml of cell suspension was transferred into each cryoprotective tubes. The cryostocks were stored at -80°C for overnight then transferred into liquid nitrogen tank for long term storage.

3.5 Calculation of N/P ratio

The N/P ratio is theoretical charge ratio between amino groups of chitosan and phosphate groups of siRNA. Amino groups have the positive charge but phosphate groups have the negative charge. The N/P ratio was appropriated that enhance efficiency transfection. The N/P ratio was calculated using follow equation:

$$\text{N/P ratio} \quad = \quad \frac{\text{nmoles N}}{\text{nmoles P}}$$

nmoles N of chitosan   = $\dfrac{\text{amount of CS (μg)}}{\text{MW of (N) CS}}$

nmoles P of siRNA   = $\dfrac{\text{amount of siRNA (μg)}}{\text{MW of (P) siRNA}}$

Average M.W. of (P) siRNA   =   333   g/mole

Average M.W. of (N) chitosan   =   161   g/mole

In this study, the amount of siRNA was fixed as 25 pmol/well in 25 μl of complexes

Stock of siRNA   =   2 μM

Stock of chitosan   =   0.44 mg/ml

Table 4. The amount of CS and siRNA per well used to form complexes at various N/P

N/P	siRNA (μl) (2μM)	CS (μl) (0.44 mg/ml)	water (μl) (DEPC)
8	12.5	3.25	9.25
16	12.5	6.25	6.25
32	12.5	12.5	-
64	12.5	12.5*	-

* CS 0.88 mg/ml

3.6 Preparation of CS/siRNA complexes

The CS/siRNA complexes were formed in DEPC water at various N/P of 8, 16,

32 and 64 by adding the siRNA solution into an equal volume of various salt form of

CS solution (Table 4). The complexes were pipetted up and down. They were then incubated for 30 min at room temperature to allow complex formation.

3.7 Characterization of CS/ siRNA complexes

3.7.1 Agarose gel electrophoresis

2% agarose gel was prepared by dissolving 0.5 g of agarose in 25 ml of Tris-borate-EDTA (TBE) (0.1 M Tris Hcl, 0.09 M boric acid, 2 nM EDTA) buffer, pH 8.3. The gel solution was warmed up in order to dissolve the agarose. 15 µl of 1 mg/ml ethidium bromide was added into the gel solution before the gel was congealed. The CS/siRNA complexes were formulated as described in section 3.6 (Table 5). CS/siRNA complexes and naked siRNA were loaded into the agarose gel in TBE buffer, pH 8.3. The volume of the sample loaded in the well was 10 µl of CS/siRNA complex solution containing 5 pmol of siRNA. The electrophoresis was carried out at 100 V for 20 min. UV transillumination of the gel was employed to visualize siRNA and the transilluminated gel was photographed using a gel documentation analyzer (Alphaimager 2200, Alpha-Innotech, CA, USA).

Table 5. The amount of CS and siRNA per well used to form 10 µl of complexes at various N/P for gel electrophoresis.

N/P	siRNA (µl) (0.4µM)	CS (µl) (0.1 mg/ml)	water (µl) (DEPC)
8	5	1.25	3.75
16	5	2.49	2.51
32	5	4.98	0.02
64	5	4.98*	0.02

* CS 0.88 mg/ml

3.7.2 Particle size and zeta-potential of the siRNA/CS complexes

The mean particle size and surface charge of the CS/siRNA complexes were determined by using the Zetasizer Nano ZS (Malvern instrument Ltd., Malvern, UK) at room temperature. To obtain the optimum scattering intensity, the CS/siRNA complexes were formed for 30 minutes and the complex were diluted with PBS/DEPC solution pH 7.2. All samples were measured in triplicate.

3.7.3 Morphology

The morphology of the CS/siRNA complexes was determined by Atomic Force Microscope (AFM) using tapping-mode AFM in air. The complexes were diluted with 0.1% DEPC water that was passed through 0.22 µm membrane filter prior to use. These samples were dropped immediately onto freshly cleaved mica and air-dried. (Wu et al. 2004 : 294-295)

3.7.4 *In vitro* transfection

In vitro transfections were performed in adherent HeLa stable cells. Briefly, the day before transfection, 8×10^3 cells in 100 ul of growth medium were plated into sterile opaque 96-well plates. Prior to transfection, the culture medium was removed from each well and the cells were washed once with PBS and the mixture of 25 µl of CS/siRNA complexes at various N/P of 8, 16, 32 and 64 and 100 ul of MEM without serum, was added onto each well and cells were incubated at 37^oC with 5% CO_2. The GFP cell fluorescence was measured before and every 24 hour after transfection using a spectrofluorophotometer (model no: AOPUS01and A153601; A Packard bioscience company, USA) with an emission and excitation wavelength at 488 and 510 nm. respectively. The transfection efficiency was calculated from the

fluorescence intensity of siRNA(+) transfected cells and siRNA(-) transfected cells performed in parallel using the following equations:

$$\% \text{ seeding variation} = \frac{(I_{average,day0} - I_{n,day0}) \times 100}{I_{average,day0}} \quad \text{Eq.1}$$

$$\text{Adjusted fluorescent intensity } (I_{ad}) = I_{n,d1-5} + \frac{(I_{n,d1-5}) \times (\% \text{ seeding variation})}{100} \quad \text{Eq.2}$$

$$\% \text{inhibition of gene expression} = \frac{(I_{average\,ad},siRNA(-) - I_{ad},siRNA(+)) \times 100}{I_{average\,ad},siRNA(-)} \quad \text{Eq.3}$$

where $I_{average,day0}$ is the average fluorescent intensity of all wells at before transfection (day 0), $I_{n,day0}$ is the fluorescent intensity of individual well at day 0, $I_{n,d1-5}$ is the fluorescent intensity at day 1-5 of each well, I_{ad} is adjusted fluorescent intensity, I_{ad},siRNA(+) is adjusted fluorescent intensity of the cell with CS/siRNA (+) complexes, and $I_{average\,ad}$,siRNA(-) is an average (n=3-5) adjusted fluorescent intensity of the cell with CS/siRNA (-) complexes.

3.7.5 Cytotoxicity of the siRNA/CS complexes

In vitro cytotoxicity test were performed in HeLa stable cells. Briefly, the day before transfection, plate 8×10^3 cells in 100 µl of growth medium into sterile 96-well plates. Prior to transfection, the culture medium was removed from each well and the cells were rinsed one time with PBS. The mixture of 25 µl of CS/siRNA complexes at various N/P of 8, 16 32 and 64 and 100 µl of MEM with no serum, was

added onto each well and the cells were incubated at 37°C and 5% CO_2. 24 post-transfection, the medium was removed and 20 µl of MTT (3-(4,5-dimethy-thiazol-2-yl)-2,5-diphenyl-tetrazolium bromide, 5 mg/ml) in serum free-medium was added to each well and the cells were incubated for 4 h to allow formation of formazan, then the medium was removed and 100 µl of DMSO was added to dissolve the formazan crystals. The absorbance of formazan was measured at 540 nm using a microplate reader (Universal Microplate Analyser, Model AOPUSO1 and A1536601, Packard bioscience company, USA). The relative cell viability was calculated by using the follow equation:

$$\% \text{ cell viability} = \frac{[OD]_{test} - [OD]_{DMSO}}{[OD]_{control} - [OD]_{DMSO}} \times 100$$

$[OD]_{test}$; value that got from wavelength 540 nm of cell which were also added siRNA /CS complexes at various N/P

$[OD]_{DMSO}$; value that got from wavelength 540 nm of cell which were also added DMSO

$[OD]_{control}$; value that got from wavelength 540 nm of cell which were not added siRNA /CS complexes

3.7.6 Statistical analysis

All experimental measurements were collected in triplicate. Result values were expressed as mean value ± standard deviation (SD).

CHAPTER IV

RESULTS AND DISCUSSION

1. Results

1.1 Complex formation of CS salt form with siRNA

Complex formation between siRNA and various CS salt forms were confirmed by gel retardation assay. When the concentration of CS gradually increased, the siRNA showed gradual retardation within the gel. The migration of siRNA on an agarose gel was retarded and depended on molecular weight and size enlargement and reduction of negative charge of chitosan/siRNA complexes (CS/siRNA) as compared to those of the free siRNA.

Figure 12 illustrated the gel retardation assay of CS-H/siRNA complexes of various MW of CS. The result showed that CS with different MW started binding to siRNA at different N/P ratio. The CS-H MW 20, CS-H MW 45, CS-H MW 200 and CS-H MW 460 showed initial binding to siRNA at N/P ratios of 8 (Figure 12a, Lane 5), 16 (Figure 12b, Lane 6), 4 (Figure 12c, Lane 4) and 32 (Figure 12d, Lane 7), respectively. The migration of siRNA in these complexes retarded as compared to the migration of unbound siRNA. (Figure 12a-d lane 1) Some of them show smear band in 2 % agarose gel due to their size variation of the CS/siRNA complexes.

Figure 13 illustrated the gel retardation assay of CS-L/siRNA complexes of various MW of chitosan. The result showed that CS-L with MW of 20 and 200 kDa showed retardation in migration. The CS-L MW 20 and 200 kDa started retardation in migration at N/P ratios of 32 (Figure 13a, Lane 7) and 8 (Figure 13c, Lane 5),

respectively, whereas the CS-L with MW of 45 and 460 kDa showed no retardation (Figure 13b, Figure 13d).

Figure 14 illustrated the gel retardation assay of CS-A/siRNA complexes of various MW of chitosan. The result showed that each of MW of CS started retardation in migration at different N/P ratio. The CS-A MW 45, 200 and 460 kDa showed at N/P ratios of 8 (Figure 14b, Lane 5), 4 (Figure 14c, Lane 4) and 4 (Figure 14d, Lane 4), respectively, whereas the CS-A MW 20 kDa showed no binding to siRNA and therefore displayed no retardation (Figure 14a).

Figure 15 illustrated the gel retardation assay of CS-G/siRNA complexes of various MW of chitosan. The result showed that each of MW of CS started retardation in migration at different N/P ratio. The CS-G MW 20, 45 and 200 kDa showed at N/P ratios of 32 (Figure 15a, Lane 7), 8 (Figure 15b, Lane 5) and 64 (Figure 15c, Lane 8), respectively, whereas the CS-G MW 460 kDa showed no binding to siRNA and therefore displayed no retardation (Figure 15d).

1 2 3 4 5 6 7 8   1 2 3 4 5 6 7 8
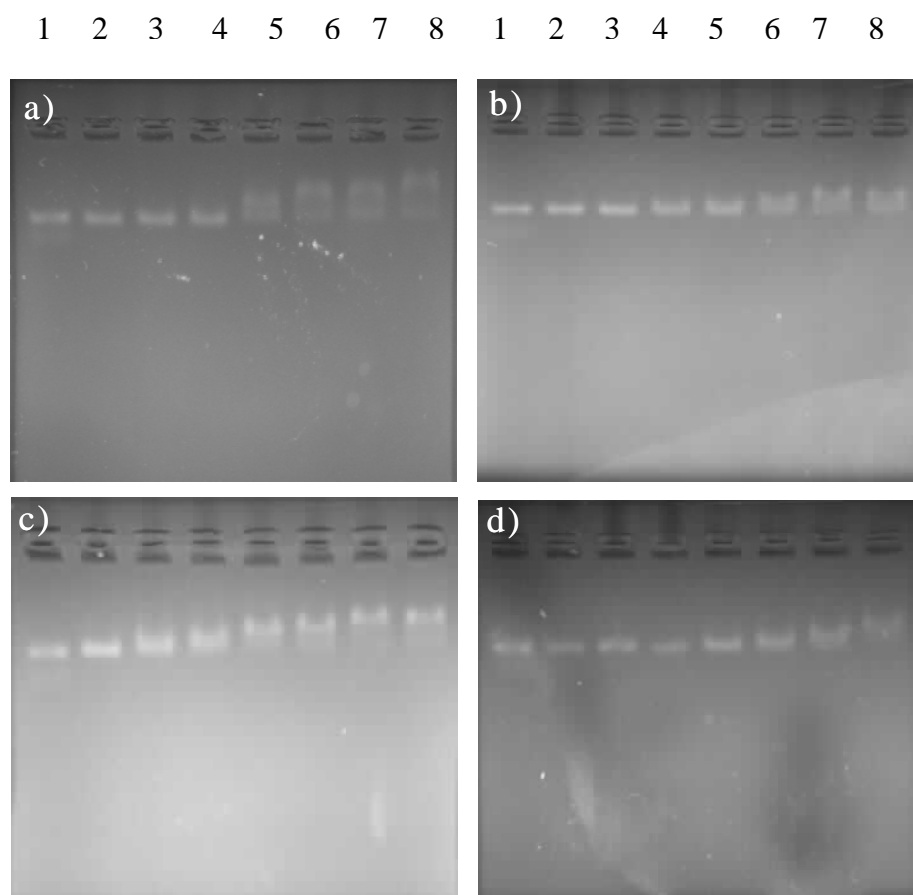
Figure 12   Gel retardation assay of CS-H/siRNA complex on 2% agarose gel. (lane 1)

siRNA-GFP (lane 2-8) N/P ratio of 1, 2, 4, 8, 16, 32 and 64 respectively.

(a) MW 20 kDa (b) MW 45 kDa (c) MW 200 kDa (d) MW 460 kDa.
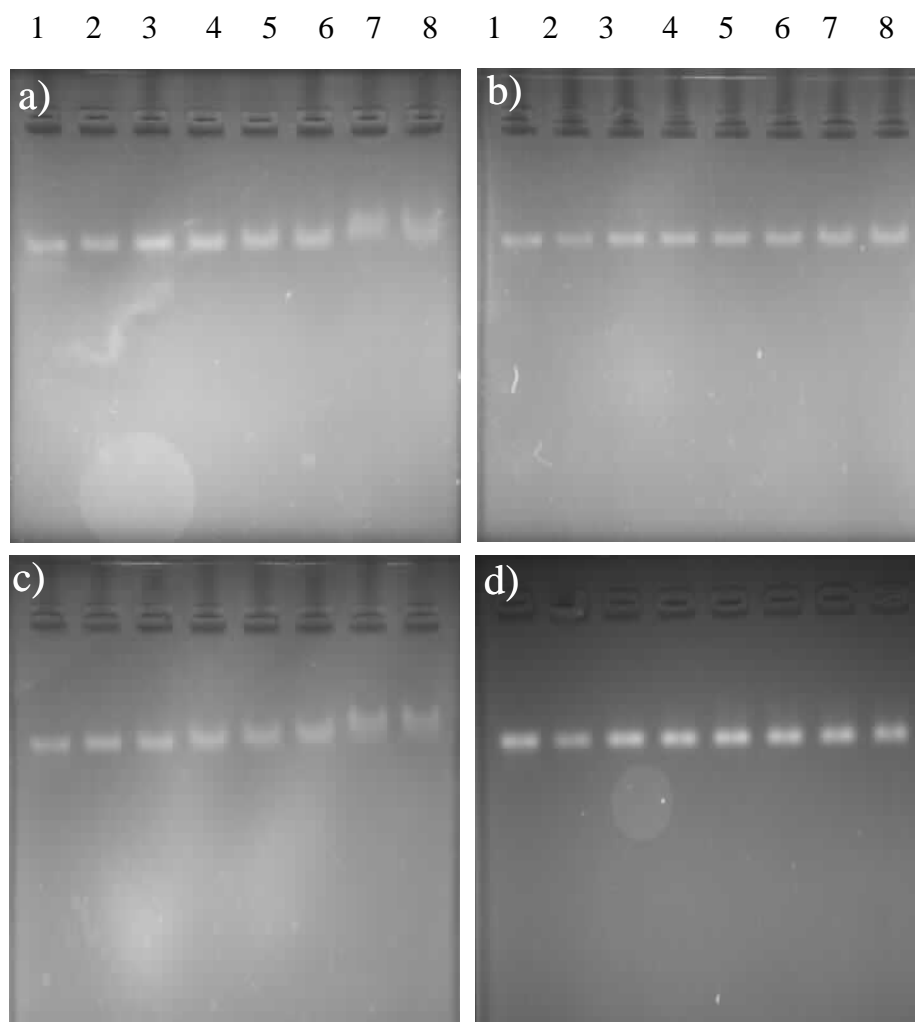
Figure 13 Gel retardation assay of CS-L/siRNA complex on 2% agarose gel. (lane 1)

siRNA-GFP (lane 2-8) N/P ratio of 1, 2, 4, 8, 16, 32 and 64 respectively.

(a) MW 20 kDa (b) MW 45 kDa (c) MW 200 kDa (d) MW 460 kDa.
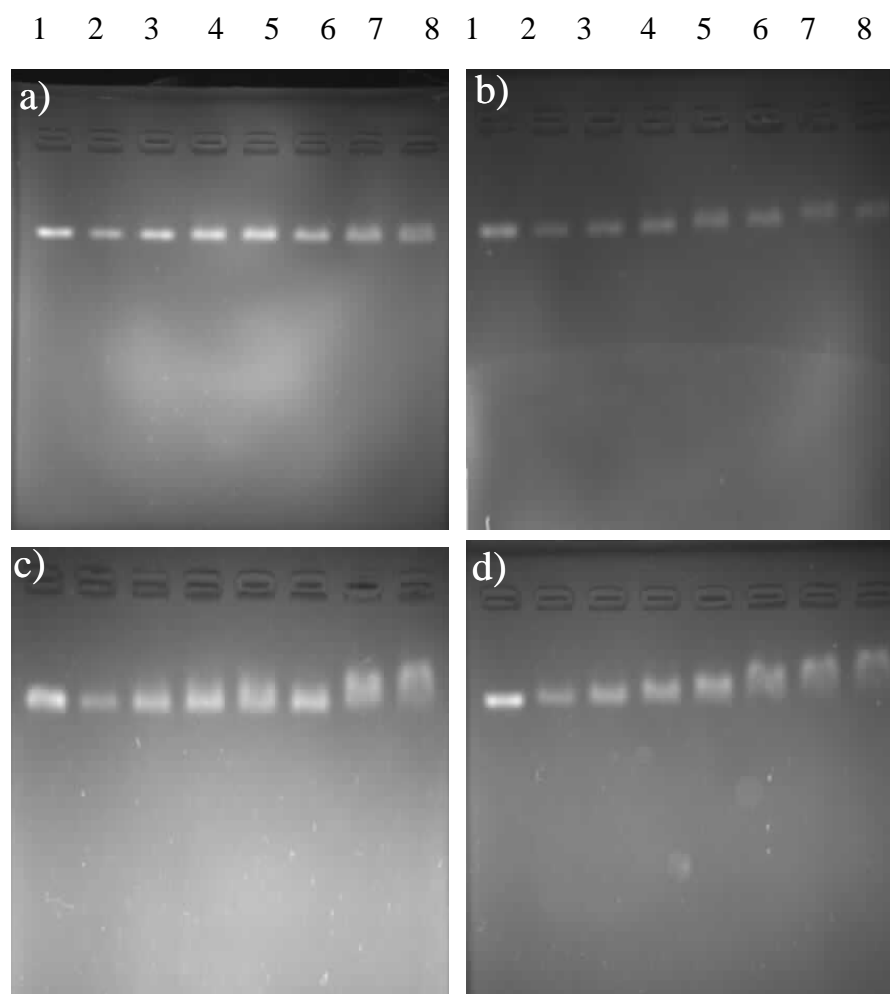
Figure 14 Gel retardation assay of CS-A/siRNA complex on 2% agarose gel. (lane 1)

siRNA-GFP (lane 2-8) N/P ratio of 1, 2, 4, 8, 16, 32 and 64 respectively.

(a) MW 20 kDa (b) MW 45 kDa (c) MW 200 kDa (d) MW 460 kDa.
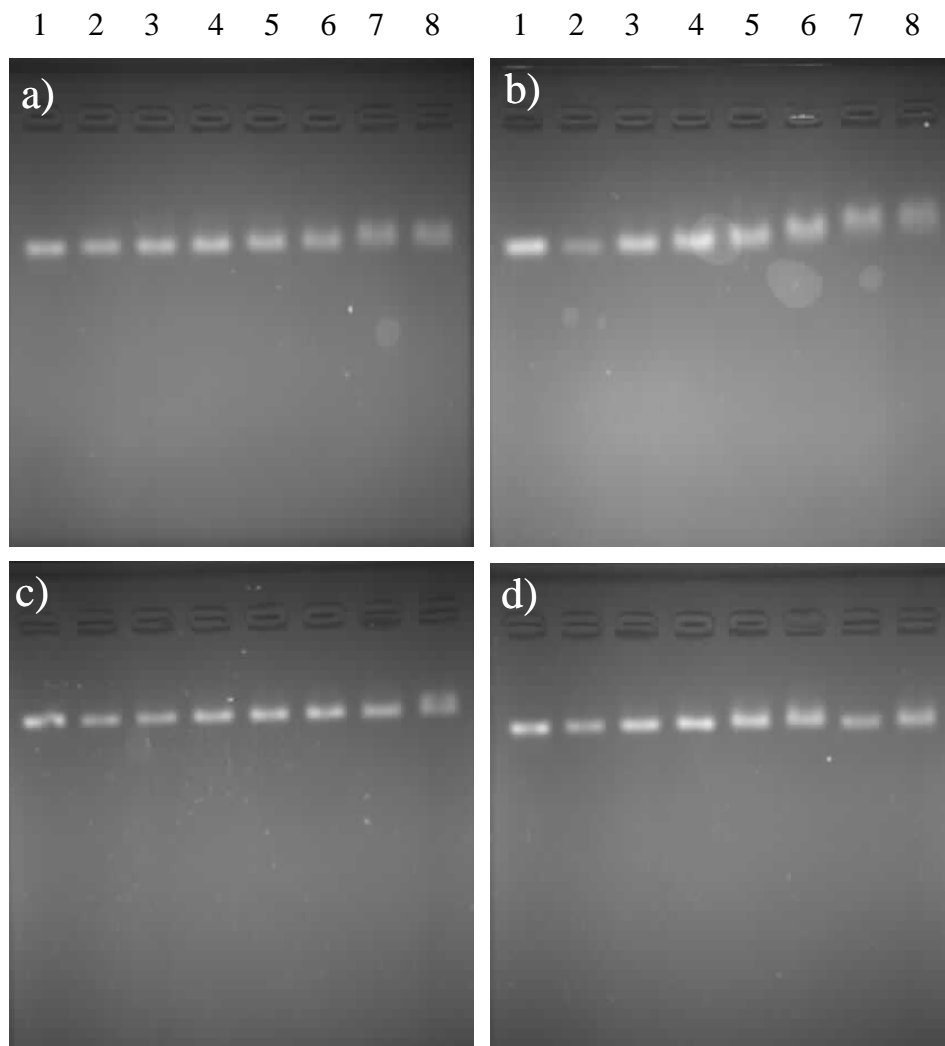
Figure 15   Gel retardation assay of CS-G/siRNA complex on 2% agarose gel. (lane 1)

siRNA-GFP (lane 2-8) N/P ratio of 1, 2, 4, 8, 16, 32 and 64 respectively.

(a) MW 20 kDa (b) MW 45 kDa (c) MW 200 kDa (d) MW 460 kDa.

1.2 The particle size and zeta-potential of the CS/siRNA complexes

      1.2.1 The particle size and zeta-potential of the CS-H/siRNA complexes

      The particle size and zeta-potential of the CS-H/siRNA complexes of various MW (20, 45, 200 and 460 kDa) at N/P ratio 8, 16, 32 and 64 are shown in Figure 16. MW of CS did not significantly affect the particle size and zeta potential. The zeta-potential of all CS-H/siRNA complexes slightly increased toward positive charge with an increasing N/P ratio. At the N/P ratio 8 and 16, the complexes had negative surface charge, whereas the complexes at N/P ratio 32 and 64 had neutral to slightly positive surface charge. The particle sizes of all complexes were in nanometer (less than 500 nm).

      1.2.2 The particle size and zeta-potential of the CS-L/siRNA complexes

      The particle size and zeta-potential of the CS-L/siRNA complexes of various MW (20, 45, 200 and 460 kDa) at N/P ratio 8, 16, 32 and 64 are shown in Figure 17. MW of CS did not significantly affect the particle size and zeta potential. The zeta-potential of all CS-L/siRNA complexes slightly increased toward positive charge with an increasing N/P ratio. At the N/P ratio 8 and 16, the complexes had negative surface charge. Whereas the complexes at N/P ratio 32 and 64 had neutral to slightly positive surface charge. The particle sizes of all complexes were in nanometer (less than 600 nm).

1.2.3 The particle size and zeta-potential of the CS-A/siRNA complexes

The particle size and zeta-potential of the CS-A/siRNA complexes of various MW (20, 45, 200 and 460 kDa) at N/P ratio 8, 16, 32 and 64 are shown in Figure 18. MW of CS did not significantly affect the particle size and zeta potential. The zeta-potential of all CS-A/siRNA complexes slightly increased toward positive charge with an increasing N/P ratio. At the N/P ratio 8 and 16, the complexes had negative surface charge. Whereas the complexes at N/P ratio 32 and 64 had neutral to slightly positive surface charge. The particle sizes of all complexes were less than 500 nm except the CS-A/siRNA complexes at N/P ratio 16 of CS MW 460 kDa was 879 nm.

1.2.4 The particle size and zeta-potential of the CS-G/siRNA complexes

The particle size and zeta-potential of the CS-G/siRNA complexes of various MW (20, 45, 200 and 460 kDa) at N/P ratio 8, 16, 32 and 64 are shown in Figure 19. MW of CS did not significantly affect the particle size and zeta potential. The zeta-potential of all CS-G/siRNA complexes slightly increased toward positive charge with an increasing N/P ratio. At the N/P ratio 8 and 16, the complexes had negative surface charge. Whereas the complexes at N/P ratio 32 and 64 had neutral to slightly positive surface charge. The particle sizes of all complexes were less than 600 nm except for the CS-G/siRNA complexes at N/P ratio 32 of CS MW 20 kDa was 850 nm.
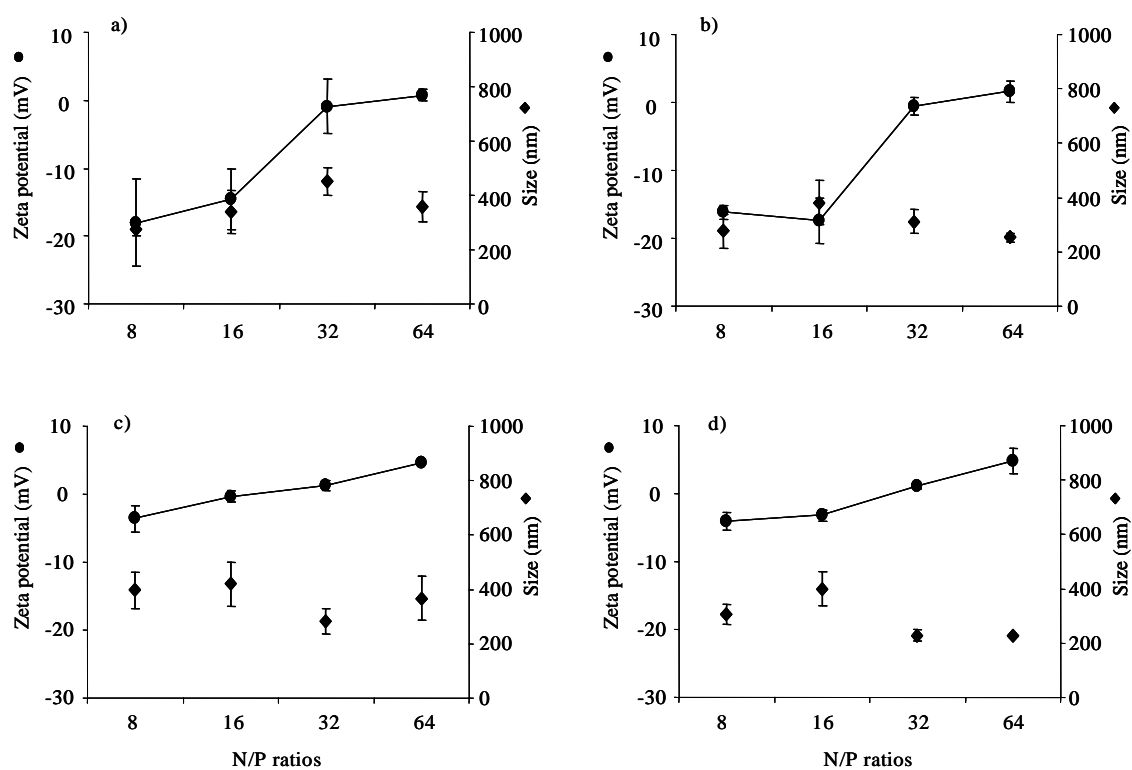
Figure 16 Particle size (♦) and zeta potential (●) of CS-H/siRNA complex of CS

various MW (a) MW 20 kDa (b) MW 45 kDa (c) MW 200 kDa and (d)

MW 460 kDa at varying N/P ratios.
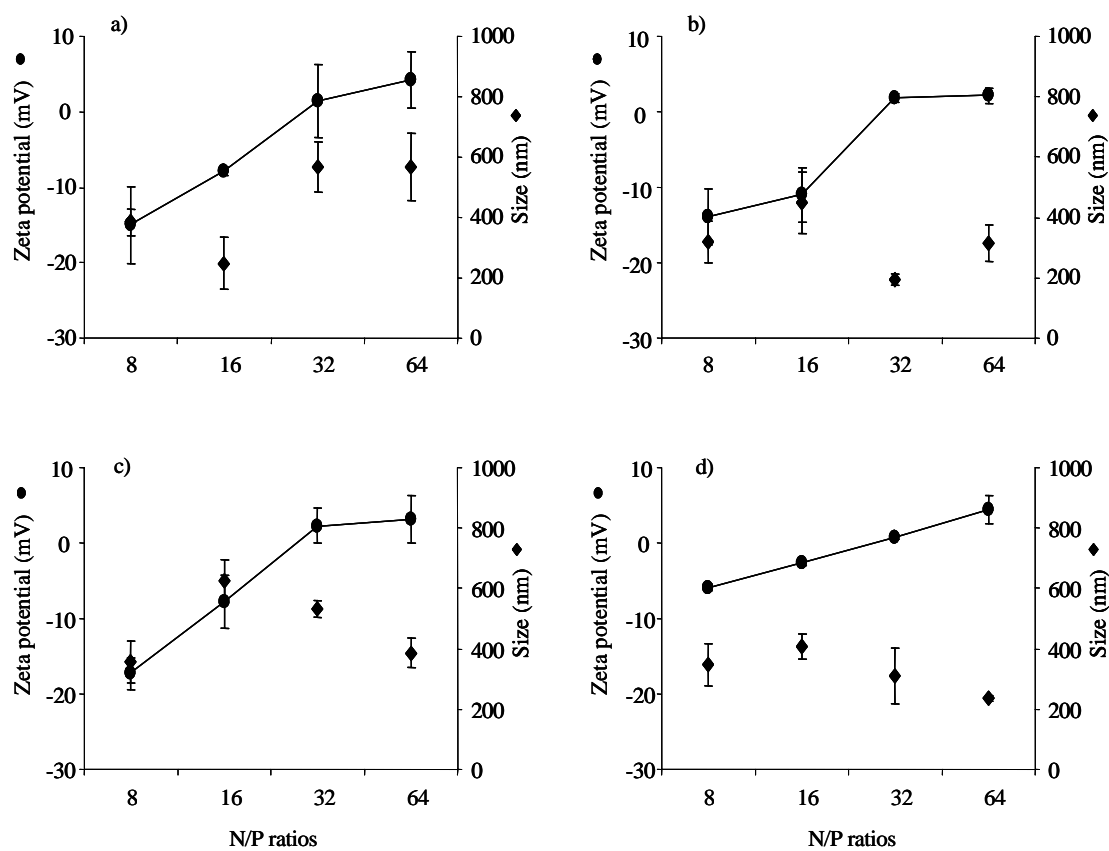
Figure 17 Particle size (♦) and zeta potential (●) of CS-L/siRNA complex of CS various MW (a) MW 20 kDa (b) MW 45 kDa (c) MW 200 kDa and (d) MW 460 kDa at varying N/P ratios.
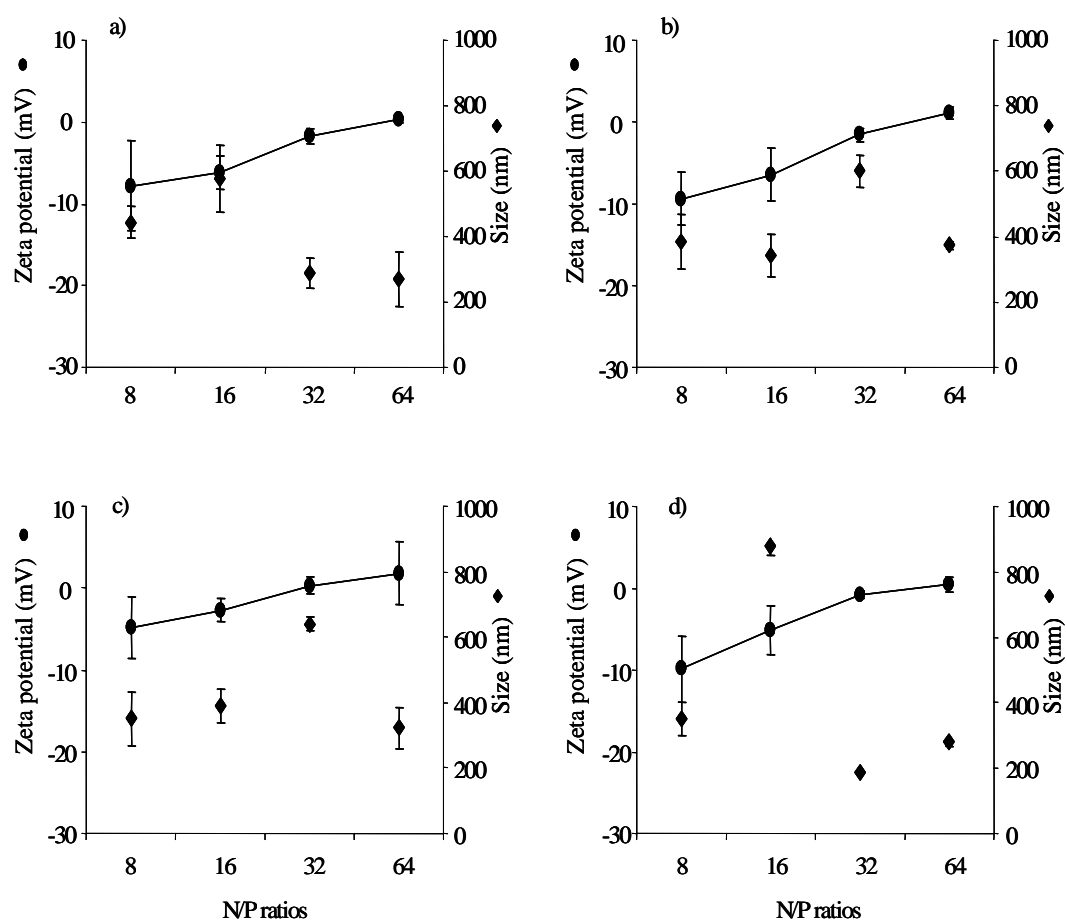
Figure 18 Particle size (♦) and zeta potential (●) of CS-A/siRNA complex of CS

various MW (a) MW 20 kDa (b) MW 45 kDa (c) MW 200 kDa and (d)

MW 460 kDa at varying N/P ratios.
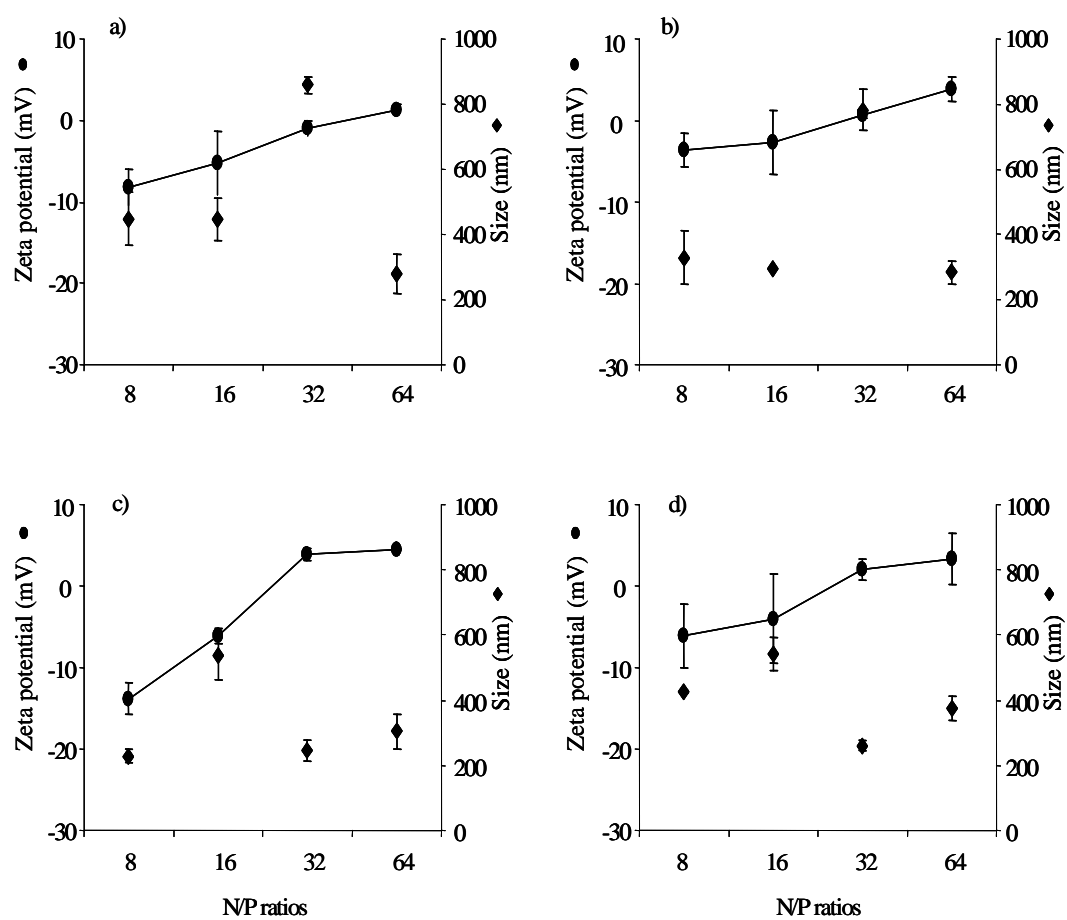
Figure 19   Particle size (♦) and zeta potential (●) of CS-G/siRNA complex of CS

various MW (a) MW 20 kDa (b) MW 45 kDa (c) MW 200 kDa and (d)

MW 460 kDa at varying N/P ratios.

1.3 Morphology

The morphology of CS/siRNA complexes formed at N/P ratio 16 and 32 using CS-H with MW 20 kDa was studied by atomic force microscopy (AFM). The AFM images revealed that the complexes were spherical shape with size in nanometer and heterogeniety (Figure 20 A-B).
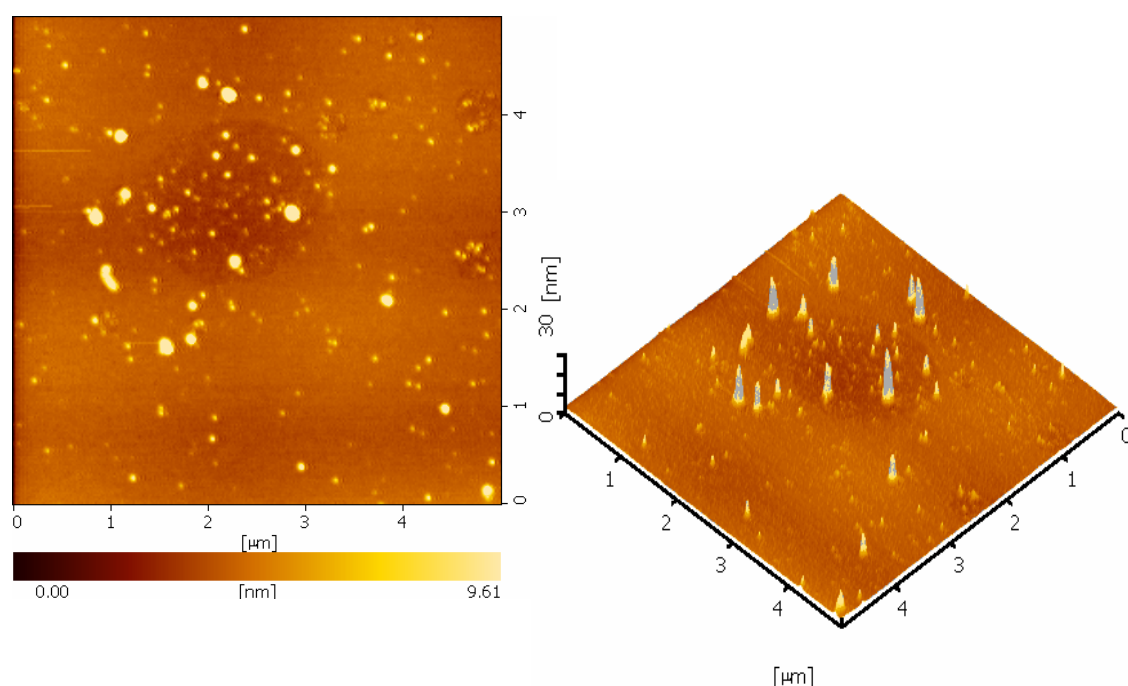
Figure 20 A   The planar and three-dimensional AFM images of complexes between

CS-H MW 20 KDa and siRNA at N/P ratio 16 (a) planar images; (b)

three-dimensional image.
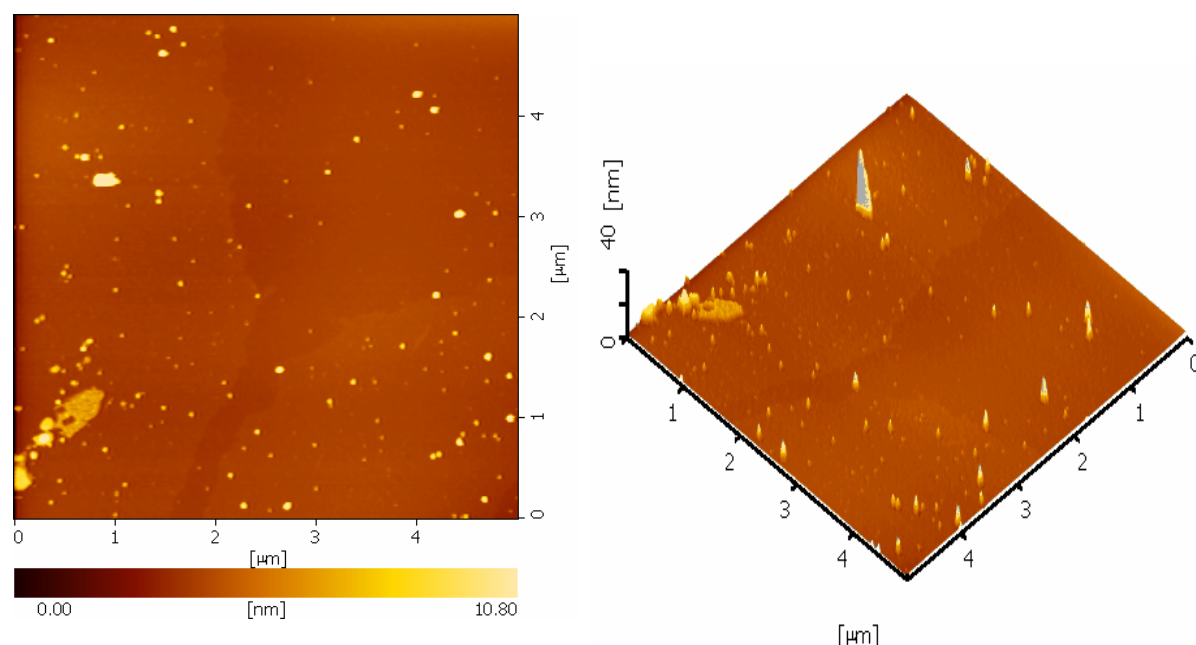
Figure 20 B The planar and three-dimensional AFM images of complex between CS-
H MW 20 KDa and siRNA at N/P ratio 32 (a) planar images; (b) three-
dimensional image.

1.4 *In vitro* **transfection**

To investigate the CS salts mediated *in vitro* siRNA transfection efficiency, siRNA transfection assay was performed in HeLa cells stable expressing green fluorescent protein (EGFP). The inhibition of GFP gene expression level was affected by transfection of CS/siRNA complexes into the stable cells. We measured EGFP expression by using Fusion Force Microscope Analyzer. Polyethyleneimine (PEI, 25 KDa) was used as a positive control. In this study, the factors including salt

form, MW and N/P ratio affecting on *in vitro* transfection efficiency were investigated.

1.4.1 Effect of CS MW and N/P ratio

1.4.1.1 CS-H

CS-H/siRNA complexes were formulated with CS-H of various MWs (20, 45, 200 and 460 kDa) in order to investigate the effect of MW on gene silencing efficiency. The gene silencing efficiencies of CS-H/siRNA complexes are shown in Figure 22. The gene silencing efficiencies of CS-H with MW 20, 45, 200 and 460 kDa were 41.2 ± 0.9 %, 23.4 ± 0.1 %, 14.6 ± 0.5 % and 24.3 ± 0.8 %, respectively. The complex formed by each MW of CS-H at various N/P ratios gave comparable gene silencing efficiency. The gene silencing efficiency of the CS-H/siRNA complexes had a tendency to decrease as the N/P ratio increased. The low MW of CS-H showed higher gene silencing efficiency than the high MW of CS-H. CS-H MW 460 kDa gave the similar gene silencing efficiency to CS-H MW 45 kDa. The maximum gene silencing efficiency was found in different N/P ratios studied. The CS-H/siRNA complexes of MW 20, 45, 200 and 460 kDa showed maximum gene silencing efficiency at N/P ratios of 8, 8, 16 and 8, respectively.
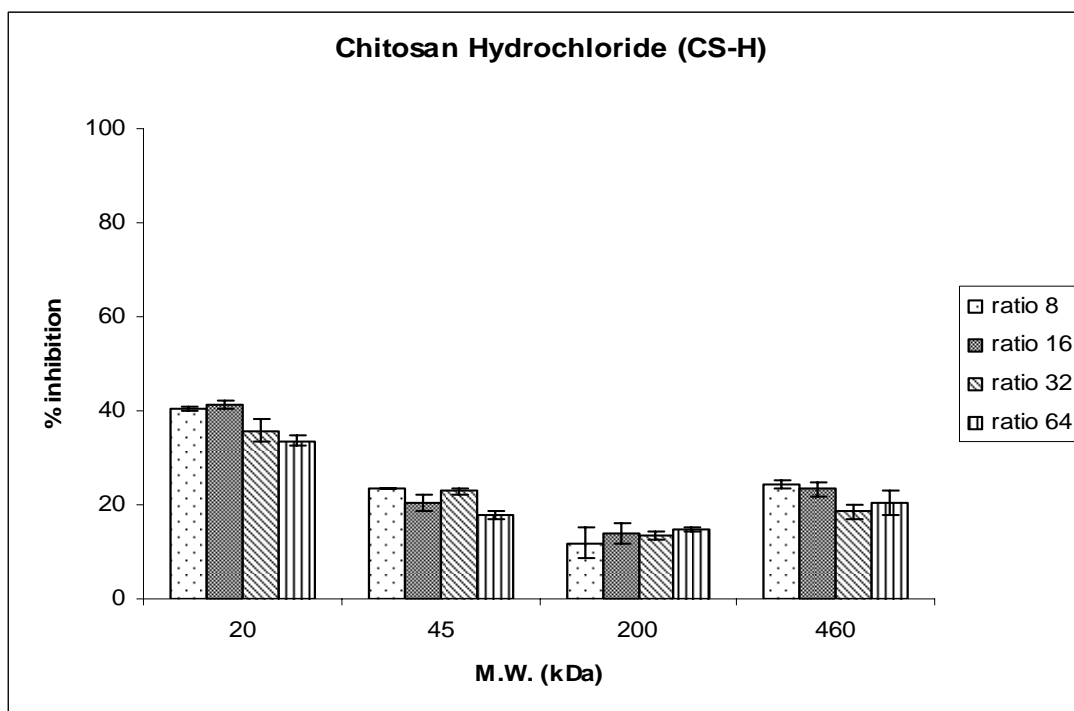
Figure 21 Effect of MW of CS and N/P ratio of CS-H/siRNA complexes on gene

silencing efficiency in HeLa stable cells (n=4).

1.4.1.2 CS-L

CS-L/siRNA complexes were formulated with CS-L of various MWs

(20, 45, 200 and 460 kDa) in order to investigate the effect of MW on gene silencing

efficiency. The gene silencing efficiencies of CS-L/siRNA complexes are shown in

Figure 23. The maximum gene silencing efficiencies of CS-L with MW 20, 45, 200

and 460 kDa were $17.0 \pm 5.1\%$, 12.4 ± 4.4 %, 6.9 ± 1.6 % and 13.0 ± 3.4 %,

respectively. The complex formed by each MW of CS-L at various N/P ratios gave

comparable gene silencing efficiency.
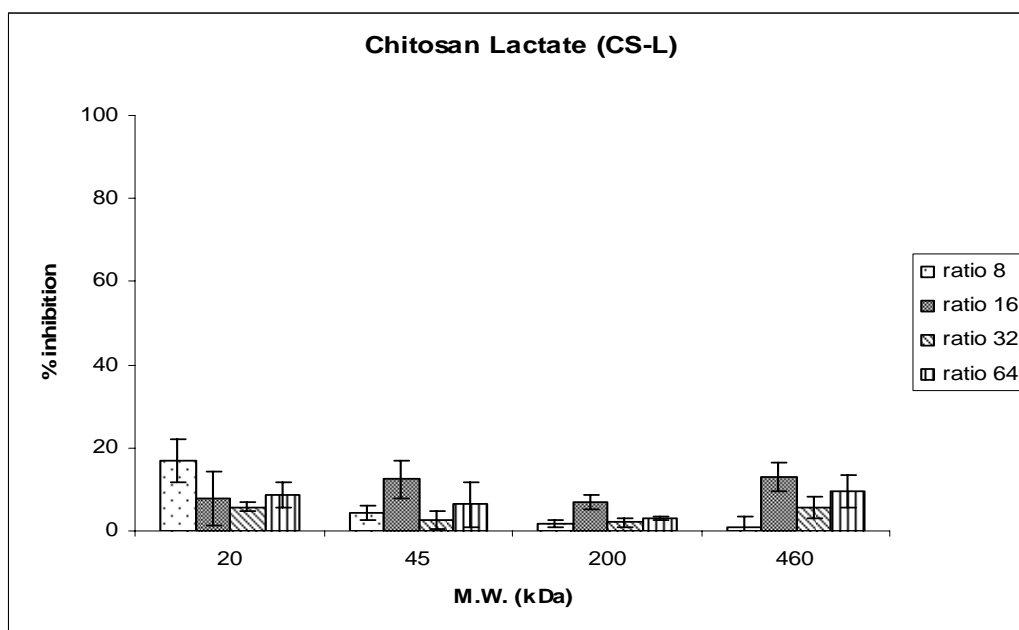
Figure 22 Effect of MW of CS and N/P ratio of CS-L/siRNA complexes on gene

silencing efficiency in HeLa stable cells (n=4).

1.4.1.3 CS-A

CS-A/siRNA complexes were formulated with CS-A of various MWs (20, 45, 200 and 460 kDa) in order to investigate the effect of MW on gene silencing efficiency. The gene silencing efficiencies of CS-A/siRNA complexes are shown in Figure 24. The maximum gene silencing efficiency of CS-A/siRNA complexes were ranked as CS-A 20 kDa (48.8%±2.3) > 45 kDa (42.8%±1.6) > 200 kDa (12.7%±3.1) > 460 (6.8%±2.1) kDa. The gene silencing efficiency had a tendency to increase as the N/P ratio increased. All MW of CS-A had maximum gene silencing efficiency at N/P ratio 64, except for MW 200 kDa had maximum gene silencing efficiency at N/P ratio 16.
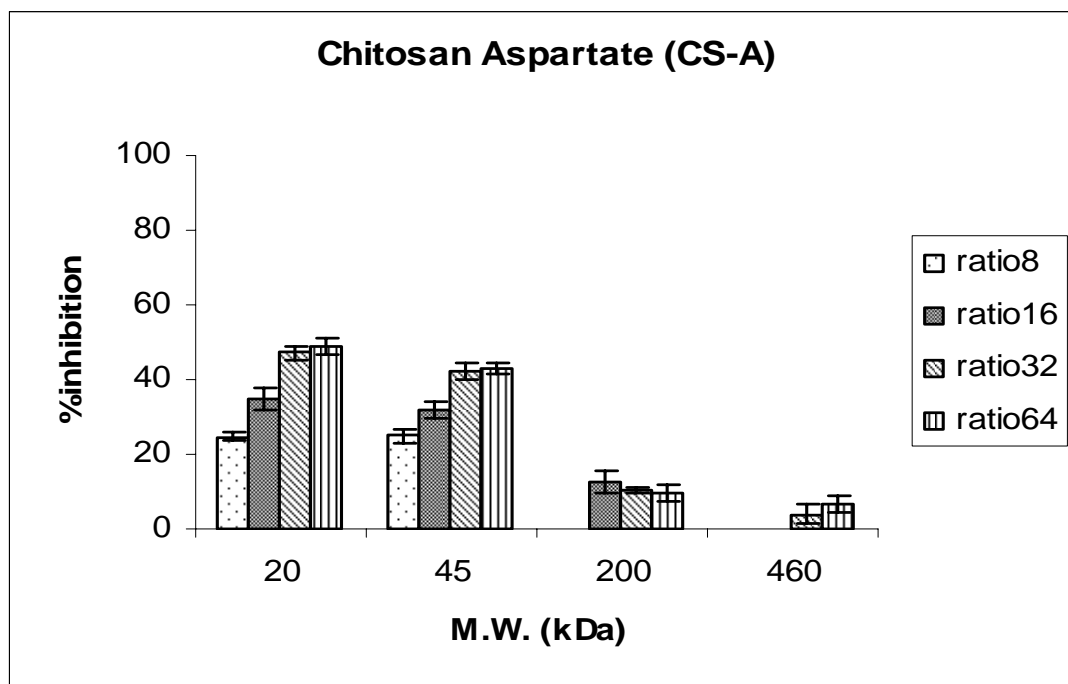
Figure 23 Effect of MW of CS and N/P ratio of CS-A/siRNA to gene silencing

efficiency in HeLa stable cells (n=5).

1.4.1.4 CS-G

CS-G/siRNA complexes were formulated with CS-G of various MWs

(20, 45, 200 and 460 kDa) in order to investigate the effect of MW on gene silencing

efficiency. The gene silencing efficiencies of CS-G/siRNA complexes are shown in

Figure 25. The gene silencing efficiency of CS-G/siRNA complexes were ranked as

CS-G 20 kDa (24.8%±1.5) > 200 kDa (20.0%±2.7) > 460 kDa (17.2%±1.5) > 45

(13.4%±4.2) kDa. The gene silencing efficiency had a tendency to increase as the N/P

ratio increased. All MW of CS-G had maximum gene silencing efficiency at N/P ratio

64.
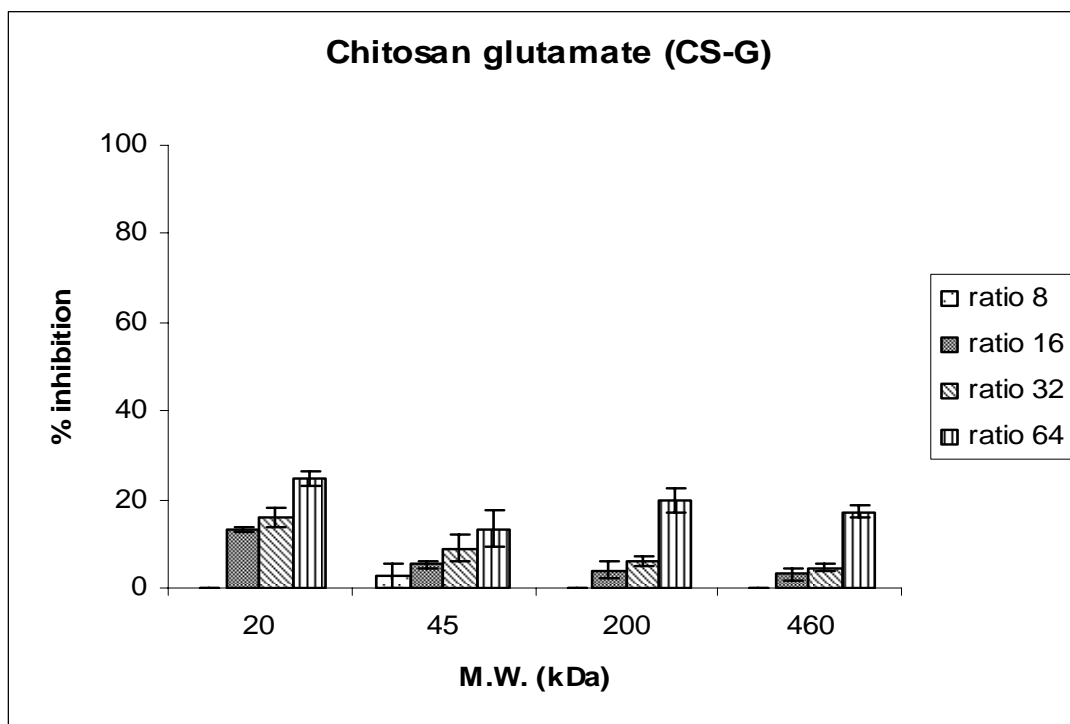
Figure 24 The effect of MW of CS and N/P ratio of CS-G/siRNA to gene silencing

efficiency in HeLa stable cells (n=5).

1.4.2 The effect of chitosan salt form

In order to investigate the effect of salt form of CS on transfection efficiency,

the CS/siRNA complexes were formulated with CS MW 20 kDa of 4 salt form

including CS-H, CS-L, CS-A and CS-G at N/P ratio of 8, 16, 32 and 64. PEI was used

as a positive control. The gene silencing efficiency of CS/siRNA complexes and

PEI/siRNA complexes were shown in Figure 21. The maximum gene silencing

efficiency of PEI/siRNA complexes at an N/P ratio of 32 was $31.7\pm1.1\%$. The

maximum gene silencing efficiency of each CS salt was found in different N/P ratios.

CS-H/siRNA, CS-L/siRNA, CS-A/siRNA and CS-G/siRNA complexes showed maximum gene silencing efficiencies at N/P ratios of 8 (34.2±0.5%), 16 (14.6±1.5), 64 (32.4±4.7) and 64 (25.8±1.1), respectively. The gene silencing efficiency of CS-H and CS-L tended to decrease when increasing N/P ratio. On the other hand, the gene silencing efficiency of CS-A and CS-G increased when increasing N/P ratio.
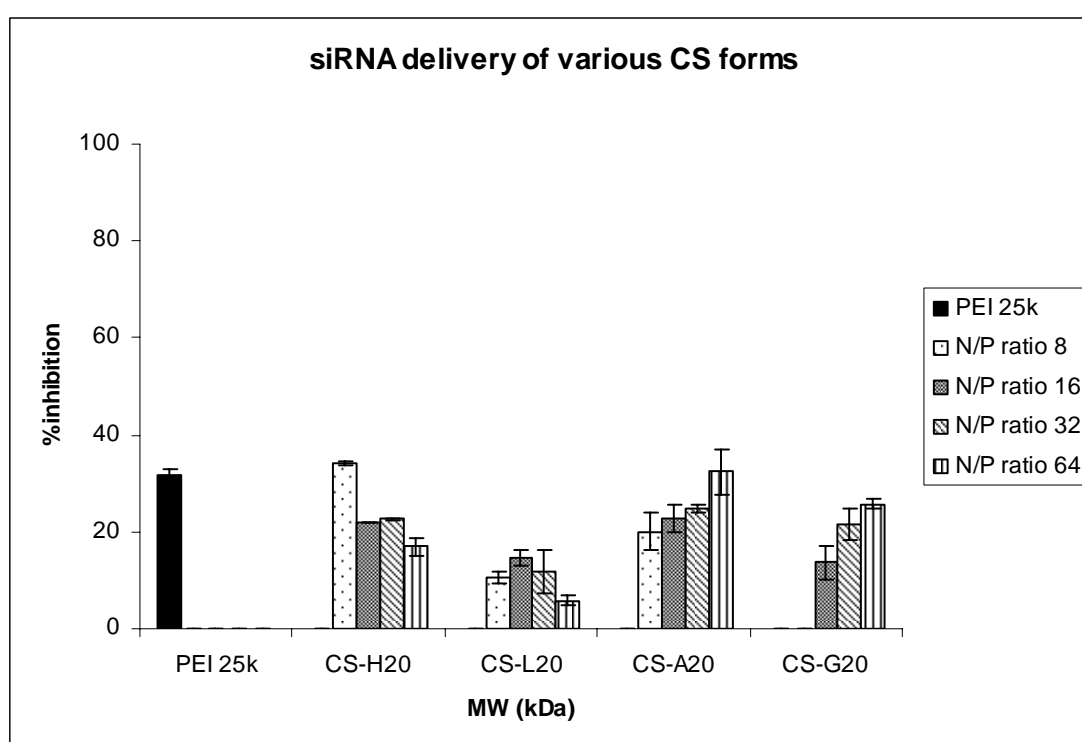
Figure 25 Percentage of GFP inhibition of CS/siRNA complexes formulated with CS
          MW 20 kDa of different salts in HeLa stable cells. Each value represents
          the mean ± S.D. of four wells.

1.5 Effect of chitosan/siRNA complexes on cell viability

A cytotoxicity assay was performed in order to evaluate the potential of CS as a vector for a safe gene delivery. Therefore, the cytotoxicity of CS-H/siRNA, CS-L/siRNA, CS-A/siRNA and CS-G/siRNA complexes at various N/P ratios was examined in HeLa stable cells. The cell viability was determined by MTT assays. Cells without treatment of the CS/siRNA complexes were considered as a control with a cell viability of 100%. The effect of CS/siRNA complexes with various CS salts, MW and N/P ratios on cell viability were shown in Figure 26-29. Over 90% average cell viability was observed for CS-H/siRNA complexes. Over 80% average cell viability was observed for CS-L/siRNA complexes. Over 75% average cell viability was observed for CS-A/siRNA and CS-G/siRNA complexes. On the other hand, the PEI 25 K/siRNA complexes have over 34% average cell viability was observed at N/P ratio 32 (Figure 30). The results showed that all CS/siRNA complexes formulated with various CS and MW were less toxic than PEI 25 K/siRNA complexes at N/P ratio 32.
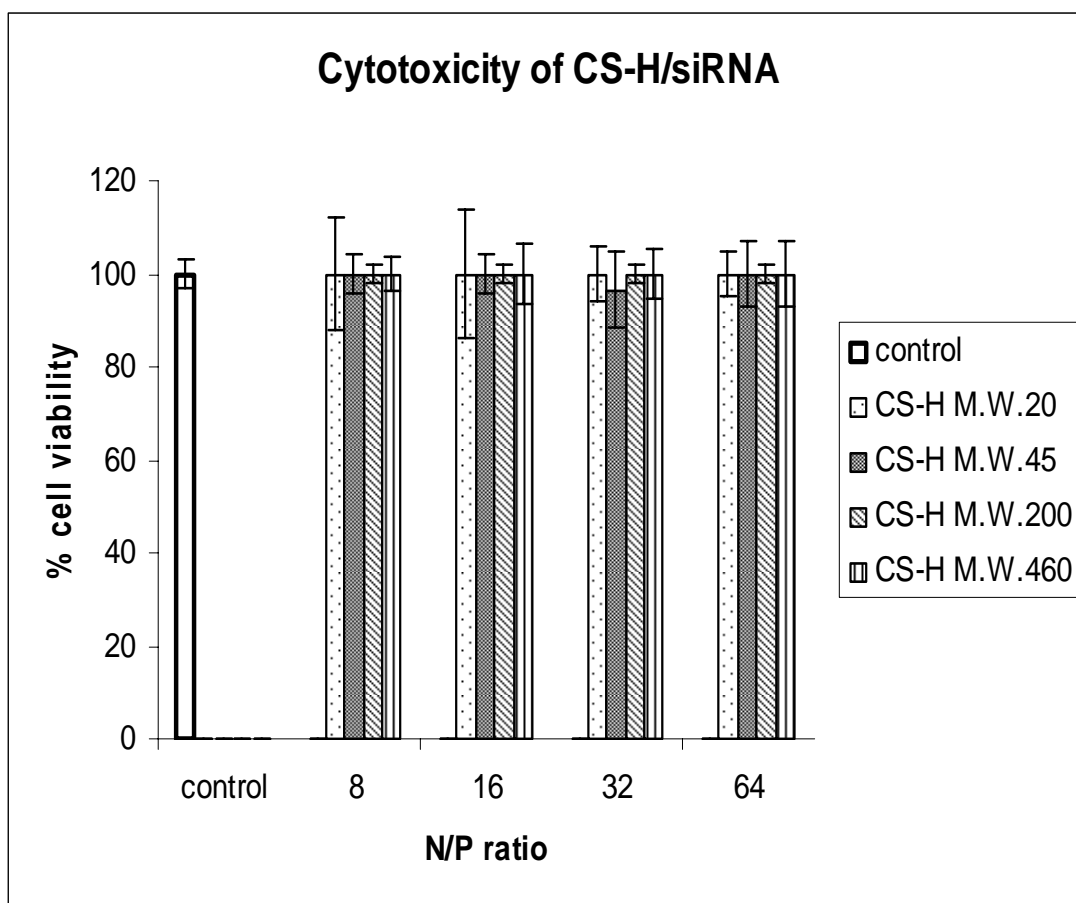
Figure 26 Effect of CS-H/siRNA complexes formulated with CS-H of different MWs (20, 45, 200 and 460 kDa) on HeLa stable cell viability (* indicated that complexes showed a significant difference from the untreated cell $p < 0.05$).
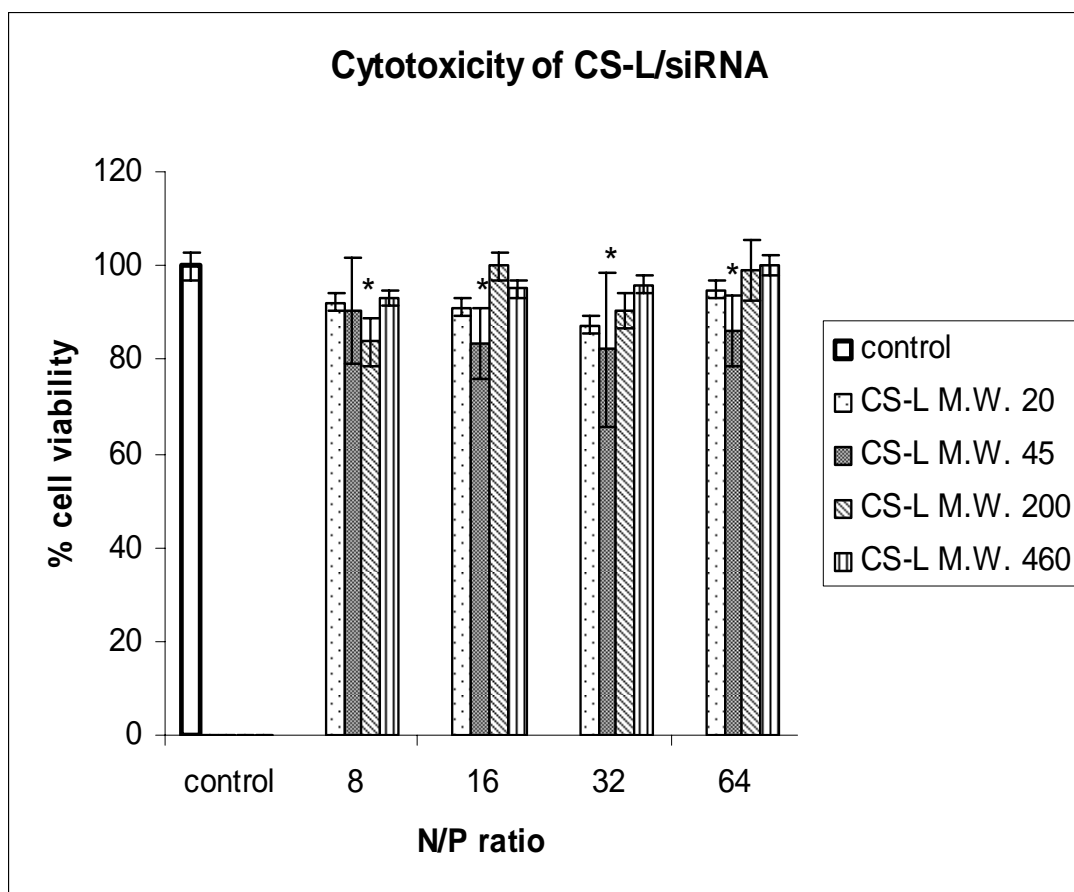
Figure 27 Effect of CS-L/siRNA complexes formulated with CS-L of different MWs

(20, 45, 200 and 460 kDa) on HeLa stable cell viability (* indicated that

complexes showed a significant difference from the untreated cell $p <$

0.05).
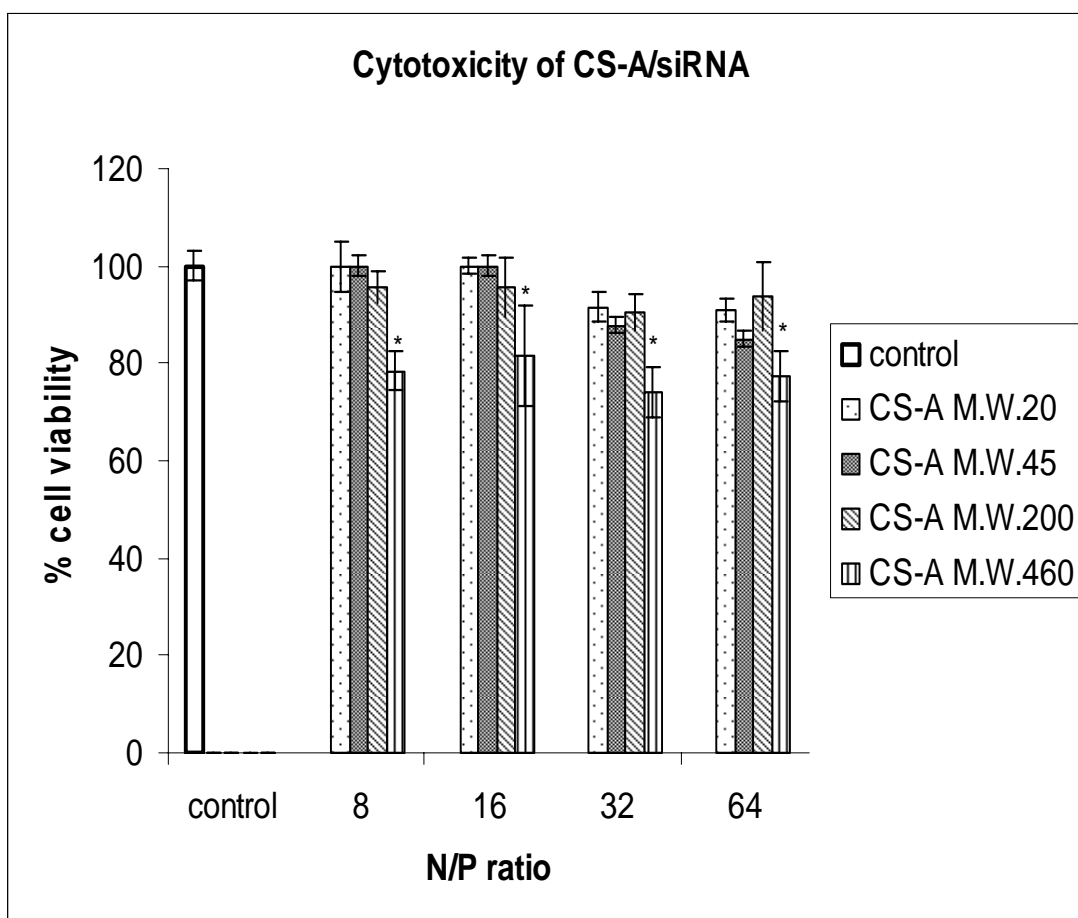
Figure 28 Effect of CS-A/siRNA complexes formulated with CS-A of different MWs

(20, 45, 200 and 460 kDa) on HeLa stable cell viability (* indicated that

complexes showed a significant difference from the untreated cell $p <$

0.05).
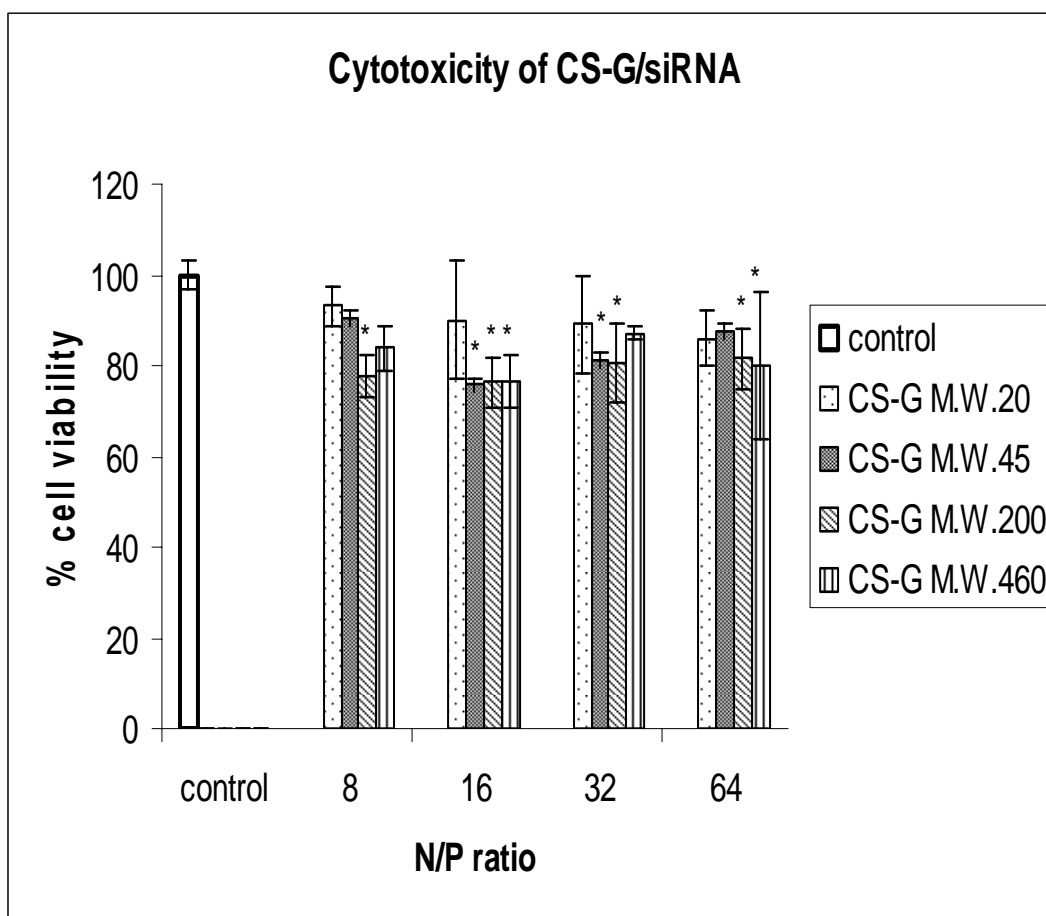
Figure 29 Effect of CS-G/siRNA complexes formulated with CS-G of different MWs

(20, 45, 200 and 460 kDa) on HeLa stable cell viability (* indicated that

complexes showed a significant difference from the untreated cell $p <$

0.05).
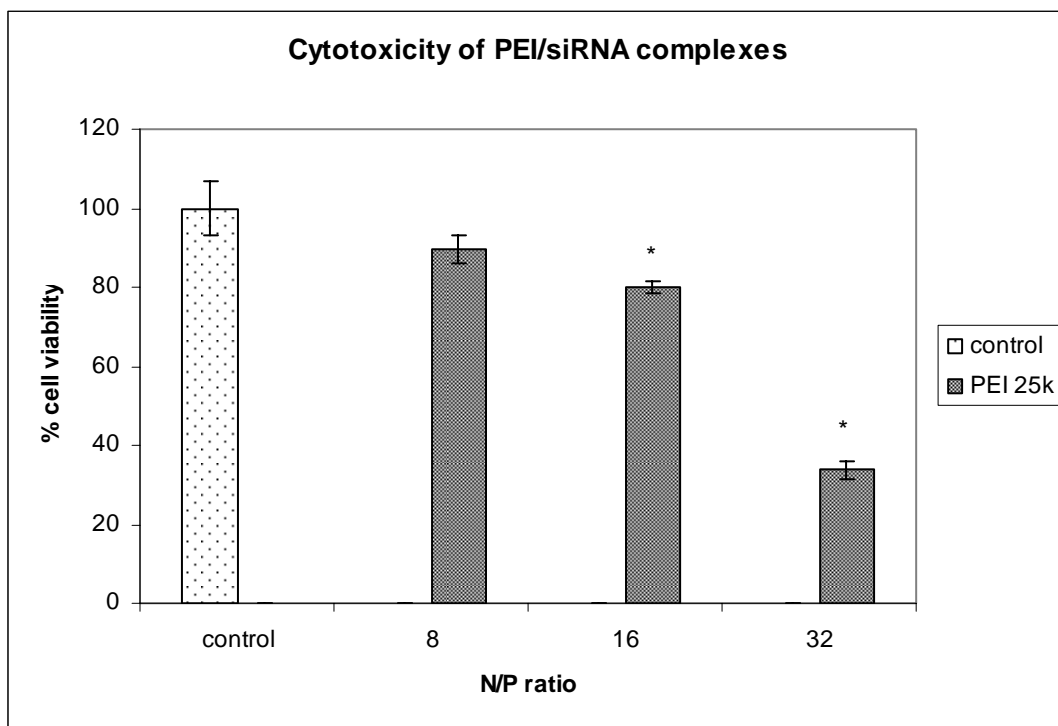
Figure 30 Effect of PEI 25k/siRNA complexes at various N/P ratio on HeLa stable

cell viability (* indicated that complexes showed a significant different

from the untreated cell $p < 0.05$).

2. Discussion

Binding of siRNA with 4 CS salt forms (CS-H, CS-L, CS-A and CS-G) and 4 MW (20, 45, 200 and 460) was investigated by gel retardation assay in 2% agarose. The migration of CS/siRNA complexes were slow down as compared to the migration of the unbound siRNA due to the size enlargement and the negative charge reduction.

Salt form and MW of CS have some effect on the interaction with siRNA. For example, CS-H with MW 20 started binding to siRNA at N/P 8 whereas CS-A with MW 20 of all N/P ratio showed no binding to siRNA. Moreover, the same CS salt with different MW start forming stable complex at different N/P ratio. For example, CS-H MW 20, CS-H MW 45, CS-H MW 200 and CS-H MW 460 showed initial binding to siRNA at N/P ratio of 8 (Figure 12a, Lane 5), 16 (Figure 12b, Lane 6), 4 (Figure 12c, Lane 4) and 32 (Figure 12d, Lane 7), respectively.

The complexes of CS/siRNA in this experiment run through 2% agarose gel as smear bands whereas the complex of CS/plasmid which remain in the well. Moreover, CS with all MW and salt forms show no binding with siRNA at N/P ratio lower than 4 indicating that siRNA required large number of CS to compact into stable complexes. This was contrary to plasmid that formed complete complex with CS at N/P ratio as low as 3 to 5. (Weecharangsan et al. 2008 : 161-168) The short length (21 bp) and the linearity of siRNA might explain the difference. This observation is in agreement with previous studies by Katas et al. and Liu et al. (Katas and Alpar 2006 : 216-225 ; Liu et al. 2007 : 1280-1288)

The effective diameters and zeta-potential of complexes formed by siRNA and various CS salt forms, MW and N/P ratios were measured. The zeta-potential of all complexes was found to increase with an increasing N/P ratio (Figure 16-19). The

increment was due to the increase in the number of positive charges which counteracts with negative charged of siRNA as the amount of siRNA was fixed. The increase in zeta-potential of CS/siRNA complexes with increasing N/P ratio or concentration of CS was also observed by Katas et al. (Katas 2006 : 216-225) A positive surface charge of complexes is necessary for binding to anionic cell surfaces by electrostatic interaction, consequently facilitating uptake of the complexes by cell. (Harush-Frenkel 2007 :26-32) While the size of all CS/siRNA complexes were in the nanometer range that had a relatively higher intracellular uptake compared to micrometer range. (Zauner 2001 : 39-51) Study in DNA, nanoparticles was advantageous in gene transfer because of enhancement of cellular uptake of the CS/DNA complexes and facilitating its subsequent release from the endo-lysosome pathway. Similar to DNA, it appeared that fine balance between the two steps of siRNA complex can enhance transfection efficiency. (Huang 2005 : 391-406)

The planar and three dimensional figure of the complexes formed by siRNA and CS-H with MW 20 at N/P ratio 16 and 32 were illustrated by AFM image (Figure 20A and 20B). The complexes were in nanometer range with size heterogeneity corresponding to the result of particle size measurement and the gel retardation assay. The complex with N/P ratio 16 showed relatively larger and less compact than the complex with N/P ratio 32 implying that siRNA bind CS looser at lower N/P ratio. The less condense complex that show weak interaction between siRNA and CS may result in better release of siRNA in the cytosol. This might partially explain the higher gene silencing activity of CS-H/siRNA complex formed at low N/P ratio (Figure 21).

Transfection of complexes of siRNA targeting EGFP gene and various CS into HeLa stable cells line expressing green fluorescent protein (EGFP) was used to

investigate the gene silencing efficiency of the various CS/siRNA complexes. The MW and N/P ratio of CS/siRNA complexes was one of the important formulation parameters that affect transfection efficiency. In the study of the effect of MW on gene silencing efficiency, CS-H/siRNA, CS-A/siRNA and CS-G/siRNA complexes of low MW chitosan of 20 kDa gave higher transfection efficiencies than the complexes of high MW chitosan of 45, 200 and 460 with an exception of CS-L. (Figure 21, 22, 23 and 24) This could be due to these low MW of CS provided an efficient balance between appropriate protection (association at outer cell) and release (dissociation at inside cell), resulting in high in vitro gene silencing efficiency. The short chain of low MW CS resulted in loose binding siRNA, therefore siRNA could escape the endosomal vesicle into the cytosal where RNAi occurred. This observation was in agreement with previous study by Liu et al. (Liu et al. 2007 : 1280-1288) It was not clear why the complexes of all lactate salts showed very low gene silencing efficiency. The only explanation could be the impurity and solubility of CS-L as gel forming was observed during the complex formation step.

The gene silencing efficiency of CS-A/siRNA and CS-G/siRNA complexes increased when increasing N/P ratio. This might be because of the larger amount of CS at higher N/P ratios yields a higher amount of positively charged complexes to successfully transfect cells. This observation was in agreement with the previous studies. The gene silencing efficiency increased at high N/P ratios (Liu et al. 2007 : 1280-1288) whereas the CS-H/siRNA complexes showed that the N/P ratio did not significantly influence the gene silencing efficiency. However, the reason for this result was not clear.

The acids used to form CS in this study can be classified into two groups; strong acid (hydrochloric acid, 100% dissociation) and weak acid (glutamic acid, pK_a 4.25 and lactic acid, pK_a 3.86 and aspartic acid, pK_a 3.65). The maximum gene silencing efficiency of each CS salt was found in different N/P ratios. CS-H/siRNA, CS-L/siRNA, CS-A/siRNA and CS-G/siRNA complexes showed maximum gene silencing efficiencies at N/P ratios of 8, 16, 64 and 64, respectively. (Figure 25) This might be resulted by the difference structure of counter ions of each salt forms that give steric hindrance to siRNA binding to CS backbone. The CS-H/siRNA complexes showed maximum gene silencing at N/P ratios less than the CS-A/siRNA complexes and the CS-G/siRNA complexes because a hydrochloric ion is smaller than an aspartic and a glutamic ion.

A good gene carrier should have low or no cytotoxicity. In this study, a standard MTT assay was used to test for cell toxicity. In principle, MTT was changed to a formazan complex by a reductase enzyme in mitochondria of a viable cell. The amount of solubilized formazan complex measured by spectrophotometry was corresponded to the number of viable cell. The cytotoxicity of cationic polymer was probably caused by polymer aggregation on cell surfaces. This impaired the important membrane function. (Jiang et al. 2007 : 273-280) The CS-H/siRNA complexes showed lower cytotoxicity than the CS-L/siRNA, CS-A/siRNA and CS-G/siRNA complexes (Figure 26-29). The difference in cytotoxic level of complexes of each salt form leave no explanation since all salt forms were naturally found inside a cell. The complexes of all CS salt forms had lower cytotoxicity than the complex of PEI 25 K (Figure 30). This might be the result of biodegradable property of CS that lead to lower cytotoxicity. (Wong et al. 2006 : 152-158)

CHAPTER V

CONCLUSIONS

The CS salt forms were successfully used for improve solubility of CS. These CS salt forms were used to assess their gene silencing efficiency and cytotoxicity on HeLa stable cells. The effect of MW, N/P ratio and type of salt form of CS on silencing efficiency and cytotoxicity were determined. The resulted of this study could be concluded as follow:

1. **Physiochemical properties of CS/siRNA complexes**

     1.1 Complex formation of CS salt forms

     Gel retardation illustrated that CS salt forms were able to form complex with siRNA. MW and salt forms of CS affected the started binding between CS and siRNA at different N/P ratio; CS-H 20 N/P ratio 8, CS-H 45 N/P ratio 16, CS-H 200 N/P ratio 4, CS-H 460 N/P ratio 4, CS-L 20 N/P ratio 32, CS-L 45 no retardation, CS-L 200 N/P ratio 8, CS-L 460 no retardation, CS-A 20 no retardation, CS-A 45 N/P ratio 8, CS-A 200 N/P ratio 4, CS-A 460 N/P ratio 4, CS-G 20 N/P ratio 32, CS-G 45 N/P ratio 8, CS-A 200 N/P ratio 64 and CS-G 460 no retardation.

Particle size and surface charge of the CS/sRNA complexes

     The CS salt forms can form complex with siRNA in nano size range. The zeta potential of all complexes at N/P ratio 32 and 64 were neutral to slightly positively surface charge.

1.2 Morphology by AFM

The moephology of CS-H/siRNA complexes at N/P ratio 16 and 32 was determined by using AFM. The AFM image showed that the complexes were spherical in shape and nano size range.

2. I*n vitro* gene silencing efficiency

2.1 N/P ratio

The gene silencing efficiency of CS/siRNA complexes was significantly influenced by N/P ratio. By increasing N/P ratios, gene silencing efficiency of the CS-A/siRNA and CA-G/siRNA complexes had a tendency to increase. Whereas the gene silencing efficiency of the CS-H/siRNA and CS-L/siRNA complexes had a tendency to decrease as the N/P ratio increased.

2.2 Effect of Molecular weight

The gene silencing efficiency of CS/siRNA complexes was significantly influenced by MW of CS. CS-H, CS-A and CS-G showed that low MW CS (20 kDa) gave a higher gene silencing efficiency than at high MW of CS. Whereas MW of CS-L was not affected gene silencing efficiency.

2.3 Effect of salt form

The gene silencing efficiency of CS/siRNA complexes was significantly influenced by type of CS salt form. The maximum gene silencing efficiency was ranked as CS-H ~ CS-A > CS-G > CS-L.

3. Cytotoxicity

The cytotoxicity of CS/siRNA complexes can be ranked as CS-H/siRNA < CS-L/siRNA < CS-A/siRNA ~CS-G/siRNA < PEI 25 K.

BIBLIOGRAPHY

Aigner, A. "Gene silencing through RNA interference (RNAi) in vivo:Strategies based on the direct application of siRNAs." Journal of Biotechology 124 (2006) : 12-25.

Akinc, A. et al. "Exploring polyethylenimine-mediated DNA transfection and the proton sponge hypothesis." The Journal of Gene Medicine 7 (2005) : 657-663.

Amiji, M. et al. Polymeric gene delivery principles and applications. USA: CRC PRESS, 2004.

Barton, GM. et al. "Retrovirus delivery of small interfering RNA into primary cells." PNAS 23 (2002) : 14943-14945.

Bettinger, T.et al. "Peptide-mediated RNA delivery: a novel approach for enhanced transfection of primary and post-mitotic cells." Nucleic Acids Research 29 (18) (2001) : 3882-3891.

Brummelkamp, T. R. et al. "Stable suppression of tumorigenicity by virus-mediated RNA interference." Cancer Cell 2 (2002) : 243-247.

Dalby, B. et al. "Advanced transfection with lipofectamine2000 reagent: primary neurons, siRNA, and high-throughput applications." Methods 33 (2004) : 95-103.

Davis, SS. and Illum, L. "Absorption enhancers for nasal drug delivery." Clinical Pharmacokinetics 42 (2003) : 1107-1128.

Elbashir, S.M. et al. "Duplexes of 21-nucleotide RNAs mediate RNA interference in cultured mammalian cells." Nature 411 (2001) : 494-498.

Felgner, P.L. et al. "Nomenclature for synthetic gene delivery systems." <u>Human Gene Therapy</u> 8 (1997) : 511-512.

Fire, A. et al. "Potent and specific genetic interference by double-stranded RNA in *Caenorhabditis elegans*." <u>Nature</u> 391 (1998) : 806-811.

Gil, J. et al. "Induction of apoptosis by the dsRNA-dependent protein kinase (PKR)." Mechanism of action, <u>Apoptosis</u> 5 (2000) :107-114.

Grayson, A.C.R. et al. "Biophysical and structural characterization of polyethylenimine-mediated siRNA delivery *in vitro*." <u>Pharmaceutical Research</u> 23 (2006) : 1868-1876.

Hannon, G.J. "RNA interference." <u>Nature</u> 418 (2002) : 244-251.

Harish Prashanth, K.V. and Tharanathan, R.N. "Chitin/chitosan : modifications and their unlimited application potential-an overview." <u>Trends in food science & technology</u> 18 (2007) :117-131.

Harush-Frenkle, O. et al. "Targeting of nanoparticles to the clathrin-mediated endocytic pathway." <u>Biochemical Biophysical Research Communications</u> 1 (2007) : 26-32.

Huang, M. et al. "Transfection efficiency of chitosan vectors : Effect of polymer molecular weight and degree of deacetylation." <u>Journal of Controlled Release</u> 106 (2005) : 391-406.

Jiang, H.L. et al. "Chitosan-graft-polyethylenimine as a gene carrier." <u>Journal of Controlled Release</u> 117 (2007) : 273-280.

Katas H, Alpar H.O. "Development and characterisation of chitosan nanoparticles For siRNA delivery." Journal of Controlled Release 115 (2006) : 216-225.

Khoury, M. et al. "Efficient new cationic liposome formulation for systemic delivery of small interfering RNA silencing tumor necrosis factor α in experimental arthritis." Arthritis Rheum 54 (2006) : 1867-1877.

Liu, X. et al. "The influence of polymeric properties on chitosan/siRNA nanoparticle formulation and gene silencing." Biomatrials 28 (2007) : 1280-1288.

Malone, R.W. et al. "Cationic liposome-mediated RNA transfection." The National Academy of science U.S.A. 86 (1989) : 6077-6081.

Mansouri, S. et al. "Chitosan-DNA nanoparticles as non-viral vectors in gene therapy : strategies to improve transfection efficacy." European Journal of Pharmaceutics and Biopharmaceutics 57 (2004) : 1-8.

Raghuvis, S.T. et al. "Use of adeno-associated viral vector for delivery of small interfering RNA." Oncogene 22 (2003) : 5712-5715.

Ritthidej, G.C., T. Phaechamud, and T. Koizumi. "Moist heat treatment on physicochemical change of chitosan salt films." International Journal of Pharmaceutics 232 (2002) : 11-22.

Skaugrud, O. "Chitosan makes the grade." Manufacturing. Chemist 60 (1989) :31-35.

Sung, K and Chong K. "Water-soluble chitosan-based antisense oligodeoxynucleotide of interleukin-5 for treatment of allergic rhinitis." Biomaterial 28 (2007) : 3360-3368.

Stewart, SA. et al. "Lentivirus-delivered stable gene silencing by RNAi in primary cells." RNA 4 (2003) : 493-501.

Thanou, M. et al. "Quaternized chitosan oligomers as novel gene delivery vectors in epithelial cell lines." Biomaterials 23 (2002) : 153-159.

Weecharangsan, W. et al "Evaluation of chitosan salts as non-viral gene vectors in CHO-K1 cells." International Journal of Pharmaceutics 348 (2008) : 161-168.

Werth, S. et al. "A low molecular weight fraction of polyethylenimine (PEI) displays increased transfection efficiency of DNA and siRNA in fresh or lyophilized complexes." Journal of Controlled Release 112 (2006) : 257-270.

Wong, K. et al. "PEI-g-chitosan, a novel gene delivery system with transfection efficiency comparable to polyethylenimine in vitro and after liver administration in vivo." Bioconjugate Chem 17 (2006) : 152-158.

Wu, A. et al. "Atomic force microscope investigation of large-circle DNA molecules." Analytical Biochemistry 325 (2004) : 293-300.

Zauner, W. et al. "In vitro uptake of polystyrene micropheres: effect of particle size, cell line and cell density." Journal of Controlled Release 71 (2001) :39-51.

Zhou, J. et al. "PAMAM dendrimers for efficient siRNA delivery and potent gene silencing." Chem communication 4 (2006) :2362-2364.

APPENDIX I

Particle size and zeta-potential of the siRNA/chitosan salt form complexes

Table 6(A) Average of the particle size and zeta-potential of the CS-H20/siRNA complexes

Sample	N/P ratio	Size (d.nm.)	PdI	Zeta potential (mV)	Zeta Deviation (mV)
siRNA/CS-H 20	8	276.33	0.332	-12.29	85.60
	SD	14.10	0.11	8.90	85.60
	16	339.00	0.342	-8.98	76.27
	SD	62.23	0.04	6.40	103.60
	32	499.00	0.419	-0.89	37.93
	SD	6..36	0.19	0.60	6.60
	64	332.50	0.337	0.78	32.75
	SD	51.62	0.01	3.70	14.35

Table 6(B) Average of the particle size and zeta-potential of the CS-H45/siRNA complexes

Sample	N/P ratio	Size (d.nm.)	PdI	Zeta potential (mV)	Zeta Deviation (mV)
siRNA/CS-H 45	8	277.33	0.342	-4.83	30.57
	SD	41.01	0.06	1.10	0.85
	16	460.33	0.420	-12.40	20.43
	SD	80.61	0.05	1.02	6.80
	32	312.00	0.310	-0.58	22.57
	SD	13.46	0.01	1.29	0.57
	64	241.00	0.311	0.51	15.70
	SD	17.68	0.01	0.00	0.85

Table 6(C) Average of the particle size and zeta-potential of the CS-H200/siRNA
complexes

Sample	N/P ratio	Size (d.nm.)	PdI	Zeta poteptial (mV)	Zeta Deviation (mV)
siRNA/CS-H 200	8	396.00	0.447	-3.06	34.63
	SD	43.13	0.03	1.95	15.91
	16	479.33	0.414	-0.29	23.33
	SD	81.32	0.07	0.93	2.90
	32	282.00	0.362	0.81	43.60
	SD	50.20	0.02	0.70	18.24
	64	293.00	0.351	1.26	21.40
	SD	113.14	0.09	0.02	0.99

Table 6(D) Average of the particle size and zeta-potential of the CS-H460/siRNA
complexes

Sample	N/P ratio	Size (d.nm.)	PdI	Zeta potential (mV)	Zeta Deviation (mV)
siRNA/CS-H 460	8	306.00	0.276	-4.11	33.07
	SD	34.65	0.03	1.33	0.57
	16	366.50	0.317	-1.55	15.50
	SD	37.48	0.01	1.26	1.98
	32	218.50	0.322	0.27	30.75
	SD	13.44	0.06	1..93	3.61
	64	507.00	0.478	2.67	32.80
	SD	201.53	0.14	1.96	12.37

Table 6(E) Average of the particle size and zeta-potential of the CS-L20/siRNA complexes

Sample	N/P ratio	Size (d.nm.)	PdI	Zeta potential (mV)	Zeta Deviation (mV)
siRNA/CS-L 20	8	385.00	0.433	-14.37	30.27
	SD	14.85	0.22	10.32	11.81
	16	247.67	0.527	-10.82	19.77
	SD	7.07	0.10	5.61	1.56
	32	567.33	0.649	1.48	20.60
	SD	83.44	0.27	0.66	8.56
	64	452.00	0.888	2.52	16.80
	SD	89.10	0.08	4.65	5.23

Table 6(F) Average of the particle size and zeta-potential of the CS-L45/siRNA complexes

Sample	N/P ratio	Size (d.nm.)	PdI	Zeta potential (mV)	Zeta Deviation (mV)
siRNA/CS-L 45	8	319.67	0.320	-10.13	25.33
	SD	31.82	0.01	4.09	7.50
	16	450.00	0.333	-5.66	21.95
	SD	103.24	0.04	3.42	0.92
	32	194.00	0.429	1.83	24.87
	SD	24.04	0.00	0.49	3.46
	64	325.67	0.406	2.20	17.37
	SD	62.23	0.00	1.10	1.20

Table 6(G) Average of the particle size and zeta-potential of the CS-L200/siRNA complexes

Sample	N/P ratio	Size (d.nm.)	PdI	Zeta potential (mV)	Zeta Deviation (mV)
siRNA/CS-L 200	8	357.00	0.425	-8.35	27.67
	SD	56.57	0.10	2.84	9.05
	16	725.50	0.472	-7.48	38.70
	SD	211.42	0.02	3.42	24.18
	32	699.00	0.737	-0.93	27.15
	SD	359.92	0.06	3.23	13.93
	64	414.00	0.393	1.70	15.55
	SD	11.31	0.00	0.66	0.92

Table 6(H) Average of the particle size and zeta-potential of the CS-L460/siRNA complexes

Sample	N/P ratio	Size (d.nm.)	PdI	Zeta potential (mV)	Zeta Deviation (mV)
siRNA/CS-L 460	8	346.00	0.271	-2.53	69.90
	SD	45.25	0.0	0.51	99.77
	16	412.00	0.285	-1.02	23.45
	SD	59.40	0.02	0.34	1.77
	32	274.00	0.261	1.50	16.20
	SD	94.75	0.02	0.30	0.71
	64	204.50	0.307	3.05	16.30
	SD	37.48	0.00	1.59	1.84

Table 6(I) Average of the particle size and zeta-potential of the CS-A20/siRNA complexes

Sample	N/P ratio	Size (d.nm.)	PdI	Zeta potential (mV)	Zeta Deviation (mV)
siRNA/CS-A 20	8	443.33	0.376	-4.46	21.63
	SD	48.79	0.17	0.19	8.41
	16	576.00	0.349	-4.80	13.17
	SD	89.80	0.01	0.31	0.49
	32	290.00	0.270	-0.76	13.20
	SD	32.53	0.02	1.24	0.14
	64	270.33	0.279	0.13	14.27
	SD	15.56	0.02	0.58	1.48

Table 6(J) Average of the particle size and zeta-potential of the CS-A45/siRNA complexes

Sample	N/P ratio	Size (d.nm.)	PdI	Zeta potential (mV)	Zeta Deviation (mV)
siRNA/CS-A 45	8	358.67	0.215	-9.38	15.30
	SD	47.38	0.06	0.34	1.27
	16	344.00	0.258	-4.74	16.57
	SD	38.89	0.02	1.84	1.48
	32	534.33	0.350	-0.68	14.33
	SD	159.10	0.06	1.04	1.48
	64	539.67	0.356	-0.77	13.83
	SD	204.35	0.04	0.83	1.63

Table 6(K) Average of the particle size and zeta-potential of the CS-A200/siRNA complexes

Sample	N/P ratio	Size (d.nm.)	PdI	Zeta potential (mV)	Zeta Deviation (mV)
siRNA/CS-A 200	8	350.67	0.278	-4.79	17.47
	SD	69.30	0.01	0.21	1.27
	16	388.33	0.286	-2.52	16.47
	SD	79.90	0.00	1.87	2.55
	32	539.00	0.419	-0.17	14.37
	SD	209.30	0.04	0.98	2.19
	64	390.00	0.405	-0.71	14.53
	SD	87.68	0.15	1.93	1.20

Table 6(L) Average of the particle size and zeta-potential of the CS-A460/siRNA complexes

Sample	N/P ratio	Size (d.nm.)	PdI	Zeta potential (mV)	Zeta Deviation (mV)
siRNA/CS-A 460	8	483.33	0.322	-9.85	13.83
	SD	113.84	0.05	1.44	0.78
	16	875.00	0.822	-6.81	15.63
	SD	38.18	0.16	1.48	2.33
	32	189.67	0.356	-1.02	14.50
	SD	0.71	0.06	0.30	0.07
	64	378.67	0.548	0.83	13.53
	SD	0.71	0.00	0.95	0.00

Table 6(M) Average of the particle size and zeta-potential of the CS-G20/siRNA complexes

Sample	N/P ratio	Size (d.nm.)	PdI	Zeta potential (mV)	Zeta Deviation (mV)
siRNA/CS-G 20	8	446.67	0.196	-8.59	34.20
	SD	74.25	0.00	3.34	36.20
	16	446.00	0.323	1.11	50.73
	SD	64.35	0.01	4.29	19.23
	32	844.00	0.348	-0.98	27.70
	SD	11.31	0.02	0.45	1.91
	64	279.67	0.293	1.34	20.13
	SD	0.00	0.01	0.52	3.46

Table 6(N) Average of the particle size and zeta-potential of the CS-G45/siRNA complexes

Sample	N/P ratio	Size (d.nm.)	PdI	Zeta potential (mV)	Zeta Deviation (mV)
siRNA/CS-G 45	8	328.00	0.462	-2.29	23.17
	SD	19.80	0.13	1.14	3.54
	16	295.67	0.246	-3.10	18.03
	SD	20.30	0.15	5.48	0.35
	32	749.33	0.391	-0.70	18.23
	SD	197.28	0.02	0.70	3.82
	64	283.33	0.367	3.14	17.37
	SD	36.77	0.15	1.44	0.21

Table 6(O) Average of the particle size and zeta-potential of the CS-G200/siRNA complexes

Sample	N/P ratio	Size (d.nm.)	PdI	Zeta potential (mV)	Zeta Deviation (mV)
siRNA/CS-G 200	8	228.67	0.258	-13.89	24.37
	SD	13.44	0.04	8.30	2.12
	16	453.00	0.389	-1.83	18.70
	SD	297.60	0.05	2.02	3.25
	32	247.00	0.367	5.32	42.27
	SD	44.55	0.11	6.54	1.06
	64	305.00	0.520	1.19	22.03
	SD	280.72	0.27	0.40	4.81

Table 6(P) Average of the particle size and zeta-potential of the CS-G460/siRNA complexes

Sample	N/P ratio	Size (d.nm.)	PdI	Zeta potential (mV)	Zeta Deviation (mV)
siRNA/CS-G 460	8	523.33	0.305	-3.58	18.60
	SD	75.66	0.05	3.53	3.11
	16	675.67	0.397	0.23	32.00
	SD	151.32	0.08	1.30	6.43
	32	261.33	0.321	0.99	38.73
	SD	19.09	0.02	3.69	14.50
	64	775.00	0.491	0.11	15.20
	SD	378.30	0.14	0.58	2.33

APPENDIX II

2. In vitro transfection efficiency

2.1 Effect of MW of chitosan

Table 7(A)   Transfection efficiency of chitosan hydrochloride (CS-H) in medium
without serum, pH 7.2, day 6

Sample   fluorescent intensity values
CS-H 20 kDA

after adjusting %seeding difference (n =4) %inhibition GFP

	1	2	3	4	average	1	2	3	4	average	SD
8(+)	86452	81069	80026	92563	85027		40.0	40.8		**40.4**	0.5
8(-)	136410	131219	137773	134974	135094						
16(+)	73191	75691	75420	75331	74908	42.5	40.6	40.8	40.8	**41.2**	0.9
16(-)	135521	126599	124698	122514	127333						
32(+)	84851	82087	81753	77325	81504	33.2	35.3	35.6	39.1	**35.8**	2.5
32(-)	132015	125591	126374	123906	126972						
64(+)	91336	89632	92379	89384	90683	33.1	34.4	32.4	34.6	**33.6**	1.0
64(-)	140039	137262	135931	133137	136592						

Sample   fluorescent intensity values
CS-H 45 kDA

after adjusting %seeding difference (n =4) %inhibition GFP

	1	2	3	4	average	1	2	3	4	average	SD
8(+)	98077	105773	102023	101964	101959			23.4	23.4	**23.4**	0.0
8(-)	137267	131301	129814	134152	133134						
16(+)	101784	101164	97880	102239	100767		19.8	22.4	19.0	**20.4**	1.8
16(-)	128978	125359	122062	128276	126169						
32(+)	101025	96553	96322	98077	97994		23.2	23.4	22.0	**22.9**	0.8
32(-)	127331	125309	124039	126314	125748						
64(+)	102909	104387	104414	105964	104419	19.0	17.9	17.8	16.6	**17.8**	1.0
64(-)	129300	126283	127923	124892	127100						

Sample   fluorescent intensity values
CS-H 200 kDA

after adjusting %seeding difference (n =4)   %inhibition GFP

	1	2	3	4	average	1	2	3	4	**average**	SD
8(+)	119095	109799	111092	110780	112692	6.9	14.2	13.2	13.4	**11.9**	3.4
8(-)	126944	130582	127510	126838	127969						
16(+)	110559	106625	104428	108055	107417	11.4	14.6	16.3	13.4	**14.0**	2.1
16(-)	128823	123771	124685	122051	124833						
32(+)	105286	104229	103789	106590	104974	13.2	14.1	14.5	12.2	**13.5**	1.0
32(-)	124127	122708	118013	120614	121366						
64(+)	107029	105773	105815	106337	106239	14.0	15.0	15.0	14.6	**14.6**	0.5
64(-)	123838	124932	123081	125938	124447						

Sample   fluorescent intensity values
CS-H 460 kDA

after adjusting %seeding difference (n =4)   %inhibition GFP

	1	2	3	4	average	1	2	3	4	**average**	SD
8(+)	97730	96738	95532	95835	96459	23.3	24.1	25.1	24.8	**24.3**	0.8
8(-)	123390	130488	128362	127758	127500						
16(+)	91805	89233	87611	90290	89735	21.6	23.8	25.2	22.9	**23.4**	1.5
16(-)	116173	116202	116485	119680	117135						
32(+)	98522	95487	94322	94398	95682	16.1	18.7	19.6	19.6	**18.5**	1.7
32(-)	119147	116884	117829	115659	117380						
64(+)	109326	103803	101509	102505	104286	16.7	20.9	22.6	21.9	**20.5**	2.7
64(-)	131277	129992	132992	130546	131202						

Table 7(B) Transfection efficiency of chitosan lactate (CS-L) in medium without serum, pH 7.2, day 4

Sample CS-L 20 kDA   fluorescent intensity values

after adjusting %seeding difference (n =3)   %inhibition GFP

	1	2	3	average	1	2	3	average	SD
8(+)	106963	70642	77116	84907		20.7	13.4	**17.0**	5.1
8(-)	97794	91861	77511	89056					
16(+)	93986	82455	84125	86855	0.2	12.5	10.7	**7.8**	6.6
16(-)	98187	88566	95843	94199					
32(+)	92195	84731	83499	86808		5.1	6.4	**5.7**	1.0
32(-)	90098	90934	86704	89245					
64(+)	98672	94147	80027	90949	6.7	11.0		**8.8**	3.0
64(-)	109301	106521	101353	105725					

Sample CS-L 45 kDA   fluorescent intensity values

after adjusting %seeding difference (n =3)   %inhibition GFP

	1	2	3	average	1	2	3	average	SD
8(+)	84984	72206	87235	81475	5.6		3.1	**4.3**	1.8
8(-)	92716	86159	91141	90005					
16(+)	78740	84189	76397	79775	13.5	7.5	16.1	**12.4**	4.4
16(-)	85814	96634	90607	91018					
32(+)	101594	89284	86482	92453		1.0	4.1	**2.5**	2.2
32(-)	90604	95459	84369	90144					
64(+)	87209	86334	95725	89756	9.0	9.9	0.1	**6.3**	5.4
64(-)	100700	93828	92826	95785					

Sample   fluorescent intensity values
CS-L 200 kDA

after adjusting %seeding difference (n =3)   %inhibition GFP

	1	2	3	average	1	2	3	**average**	SD
8(+)	95356	86744	87908	90003		2.5	1.2	**1.8**	0.9
8(-)	87171	89559	90184	88971					
16(+)	84439	84771	87131	85447	8.0	7.7	5.1	**6.9**	1.6
16(-)	94002	91539	89935	91825					
32(+)	90438	88462	88839	89246	0.7	2.9	2.5	**2.0**	1.2
32(-)	92971	86763	93559	91098					
64(+)	102648	88921	88197	93255		2.7	3.5	**3.1**	0.6
64(-)	96330	83062	94819	91404					

Sample   fluorescent intensity values
CS-L 460 kDA

after adjusting %seeding difference (n =3)   %inhibition GFP

	1	2	3	average	1	2	3	**average**	SD
8(+)	81985	85529	86416	84643	4.0	-0.1	-1.2	**0.9**	2.7
8(-)	85820	83906	86557	85428					
16(+)	79639	75412	86379	80477	10.6	15.4		**13.0**	3.4
16(-)	84422	95405	87458	89095					
32(+)	79864	81419	84482	81922	7.9	6.1	2.6	**5.6**	2.7
32(-)	85725	89616	84876	86739					
64(+)	82916	83244	89421	85194	11.7	11.4	4.8	**9.3**	3.9
64(-)	88909	96476	96460	93948					

Table 7(C)   Transfection efficiency of chitosan aspartate (CS-A) in medium without serum, pH 7.2, day 5

Sample
CS-A 20 kDA

fluorescent intensity values

after adjusting %seeding difference (n =5)   %inhibition GFP

	1	2	3	4	5	average	1	2	3	4	5	average	SD
8(+)	168620	162174	140584	144047	145502	152186			26.3	24.4	23.7	**24.8**	1.3
8(-)	191639	187992	192492	188124	192996	190649							
16(+)	134606	119862	128940	115755	108965	121626		32.0		34.3	38.1	**34.8**	3.1
16(-)	191849	171021	166677	172970	178295	176162							
32(+)	110998	94440	87428	92522	90254	95129		45.3	49.4	46.4	47.7	**47.2**	1.7
32(-)	182955	170107	167256	171656	171192	172633							
64(+)	105463	98033	95490	96162	102989	99627	45.8	49.6	50.9	50.5	47.0	**48.8**	2.3
64(-)	206725	189463	191340	192479	192040	194409							

Sample
CS-A 45 kDA

fluorescent intensity values

after adjusting %seeding difference (n =5)   %inhibition GFP

	1	2	3	4	5	average	1	2	3	4	5	average	SD
8(+)	132119	133268	131814	126251	134977	131686	24.9	24.2	25.0	28.2	23.2	**25.1**	1.9
8(-)	180402	173895	175637	174508	174887	175866							
16(+)	117170	114004	119137	120419	111620	116470	31.7	33.5	30.5	29.8	34.9	**32.1**	2.1
16(-)	169176	171485	171519	172083	173051	171463							
32(+)	93635	103695	99475	102488	102156	100290	46.1	40.3	42.8	41.0	41.2	**42.3**	2.3
32(-)	168240	166197	174553	179640	180422	173810							
64(+)	104935	108753	101290	106733	103384	105019	42.9	40.8	44.9	41.9	43.7	**42.8**	1.6
64(-)	201114	172212	177834	172190	195249	183720							

Sample fluorescent intensity values
CS-A 200 kDA

after adjusting %seeding difference (n =5)   %inhibition GFP

	1	2	3	4	5	average	1	2	3	4	5	average	SD
8(+)	193106	195366	190737	194234	189076	192504	-0.8	-2.0	0.4	-1.4	1.3	**-0.5**	1.3
8(-)	196741	192634	188583	189498	190462	191584							
16(+)	171615	159853	161012	155835	161832	162029	7.5	13.8	13.2	16.0	12.8	**12.7**	3.1
16(-)	199771	184371	183182	177926	182436	185537							
32(+)	167746	164544	163008	165018	164808	165025	8.8	10.6	11.4	10.3	10.4	**10.3**	0.9
32(-)	191390	180843	181168	184335	182155	183978							
64(+)	181211	178439	171153	171673	178305	176156	7.3	8.8	12.5	12.2	8.8	**9.9**	2.3
64(-)	200487	197673	195011	193573	191036	195556							

Sample fluorescent intensity values
CS-A 460 kDA

after adjusting %seeding difference (n =5)   %inhibition GFP

	1	2	3	4	5	average	1	2	3	4	5	average	SD
8(+)	192797	192892	191084	192258	189439	191694	-4.3	-4.4	-3.4	-4.0	-2.5	**-3.7**	0.8
8(-)	182172	183789	184238	184305	189613	184823							
16(+)	172916	174954	175722	177701	177383	175735	1.1	0.0	-0.5	-1.6	-1.4	**-0.5**	1.1
16(-)	172342	175450	172681	175024	179058	174911							
32(+)	173395	170906	171953	179989	184223	176093	4.4	5.7	5.2	0.7		**4.0**	2.3
32(-)	185127	174800	180706	184055	181922	181322							
64(+)	187256	178202	182287	187768	187552	184613	5.5	10.1	8.0	5.2	5.3	**6.8**	2.1
64(-)	200547	191817	194982	199243	204128	198144							

Table 7(D)   Transfection efficiency of chitosan glutamate (CS-G) in medium without serum, pH 7.2, day 4

Sample CS-G 20 kDA   fluorescent intensity values

after adjusting %seeding difference (n =5)   %inhibition GFP

	1	2	3	4	5	average	1	2	3	4	5	average	SD
8(+)	155470	142251	141267	136420	142200	143522	-16.2	-6.3	-5.6	-2.0	-6.3	0.0	0.0
8(-)	144579	133697	128264	133696	128622	133772							
16(+)	134758	114203	108366	109321	116205	116570			13.4	12.7		13.1	0.5
16(-)	145573	120135	115756	119931	124541	125187							
32(+)	125959	107832	102191	103657	101565	108241		12.7	17.3	16.1	17.8	16.0	2.3
32(-)	142610	120082	116679	121600	116761	123546							
64(+)	130924	110190	105865	107272	113183	113487		23.1	26.1	25.1		24.8	1.5
64(-)	153973	143804	133225	144486	141090	143316							

Sample CS-G 45 kDA   fluorescent intensity values

after adjusting %seeding difference (n =5)   %inhibition GFP

	1	2	3	4	5	average	1	2	3	4	5	average	SD
8(+)	136142	132384	124671	129740	131285	130844			4.6	0.8		2.7	2.7
8(-)	129571	131369	131446	132725	128598	130742							
16(+)	114609	118161	114338	115975	115593	115735	5.7		6.0	4.6	4.9	5.3	0.6
16(-)	115042	119873	117256	129508	126204	121577							
32(+)	103213	108633	109403	111207	114286	109348	12.3	7.7	7.0			9.0	2.9
32(-)	107293	118912	113786	124309	123866	117633							
64(+)	109936	119766	113507	124257	120210	117535	19.0	11.7	16.3	8.4	11.4	13.4	4.2
64(-)	132615	127664	132710	137394	148016	135680							

Sample   fluorescent intensity values
CS-G 200 kDA

    after adjusting %seeding difference (n =5)   %inhibition GFP

	1	2	3	4	5	average	1	2	3	4	5	average	SD
8(+)	146032	117646	129175	126384	129042	129656	-25.6	-1.2	-11.1	-8.7	-11.0	0.0	0.0
8(-)	120684	111269	113660	116936	118808	116271							
16(+)	129627	114735	113382	113121	109700	116113			2.9	3.1	6.1	4.0	1.8
16(-)	131531	116621	112796	110387	112504	116768							
32(+)	90175	108529	107098	106278	105403	103497		4.6	5.9	6.6	7.4	6.1	1.2
32(-)	134646	110401	110193	105932	107797	113794							
64(+)	138524	123012	106297	113647	110813	118459			22.8	17.5	19.6	20.0	2.7
64(-)	155178	137979	127370	133257	135112	137779							

Sample   fluorescent intensity values
CS-G 460 kDA

    after adjusting %seeding difference (n =5)   %inhibition GFP

	1	2	3	4	5	average	1	2	3	4	5	average	SD
8(+)	128247	128012	132794	131327	118146	127705	-8.4	-8.2	-12.2	-11.0	0.1	0.0	0.0
8(-)	112919	118625	121335	121958	116728	118313							
16(+)	109272	112636	112736	115837	112461	112588	5.4	2.5	2.4		2.6	3.2	1.4
16(-)	117386	113371	118335	111732	116544	115474							
32(+)	108832	109242	110735	108406	108522	109148	4.8	4.5	3.2	5.2	5.1	4.6	0.8
32(-)	109933	112946	115325	118052	115523	114356							
64(+)	109912	111369	114853	110793	113118	112009	18.8	17.7	15.1	18.1	16.4	17.2	1.5
64(-)	135147	134504	131745	132492	142619	135301							

2.2 Effect of salt from of chitosan

Table 8 Transfection efficiency of various CS/siRNA complexes at 20 MW kDa in medium without serum, pH 7.2 day 5

Sample
CS-H 20 kDA   fluorescent intensity values

after adjusting %seeding difference (n =4)   %inhibition GFP

	1	2	3	4	average	1	2	3	4	average	SD
8(+)	113605	135956	148506	114832	128225	34.5			33.8	**34.2**	0.5
8(-)	181468	170196	166669	175780	173528						
16(+)	149412	144367	137613	137685	142269			22.1	22.0	**22.0**	0.0
16(-)	178696	178196	167986	181362	176560						
32(+)	134481	128841	140155	139533	135752			22.5	22.9	**22.7**	0.2
32(-)	190630	177004	177637	178295	180892						
64(+)	139798	146023	144307	146808	144234	19.5	15.9	16.9	15.4	**16.9**	1.8
64(-)	175378	171845	175679	171402	173576						

Sample
CS-L 20 kDA   fluorescent intensity values

after adjusting %seeding difference (n =4)   %inhibition GFP

	1	2	3	4	average	1	2	3	4	average	SD
8(+)	171109	169101	166801	171127	169535	9.7	10.7	12.0	9.7	**10.5**	1.1
8(-)	186598	189862	190201	191111	189443						
16(+)	147109	149505	146855	143292	146690	14.3	13.0	14.5	16.6	**14.6**	1.5
16(-)	170075	172451	176220	168274	171755						
32(+)	158806	153520	164342	145695	155591	10.1	13.1	7.0	17.5	**11.9**	4.5
32(-)	179943	168590	185124	172852	176627						
64(+)	169890	169182	167432	166293	168199	4.9	5.3	6.3	6.9	**5.8**	0.9
64(-)	170876	178390	184092	181111	178617						

Sample   fluorescent intensity values
CS-A 20 kDA

after adjusting %seeding difference (n =4)   %inhibition GFP

	1	2	3	4	average	1	2	3	4	average	SD
8(+)	136814	136868	141829	151356	141717	22.8	22.8	20.0	14.6	**20.0**	3.9
8(-)	168868	175936	179177	184988	177242						
16(+)	134595	137547	144670	160863	144419	25.3	23.7	19.7		**22.9**	2.9
16(-)	179998	170071	179503	191358	180233						
32(+)	137564	71868	136853	134896	120295	24.1		24.5	25.6	**24.7**	0.8
32(-)	169722	179115	179762	196294	181223						
64(+)	157059	138478	120520	130232	136572		27.9	37.3	32.2	**32.4**	4.7
64(-)	185187	187365	199879	195826	192064						

Sample   fluorescent intensity values
CS-G 20 kDA

after adjusting %seeding difference (n =4)   %inhibition GFP

	1	2	3	4	average	1	2	3	4	average	SD
8(+)	181462	165149	189533	184651	180199	1.9		-2.5	0.1	**0.0**	0.0
8(-)	190448	181897	185376	181956	184919						
16(+)	154904	157746	167337		159996	16.5	14.9	9.8		**13.7**	3.5
16(-)	197386	178406	184990	180983	185442						
32(+)	149397	137007	129067	128543	136003		19.3	24.0		**21.6**	3.3
32(-)	183375	174254	159815	161479	169731						
64(+)	145025	136316	132587	135229	137289		24.9	26.9	25.5	**25.8**	1.1
64(-)	185656	186632	176403	177199	181473						

Sample   fluorescent intensity values
CS-PEI 25 k

after adjusting %seeding difference (n =4)   %inhibition GFP

	1	2	3	4	average	1	2	3	4	**average**	SD
32(+)	129166	130230	130661	125950	129002	31.7	31.1	30.9	33.4	**31.7**	1.1
32(-)	182721	194596	176961	201662	188985						
cell	238444	212141	186697	215154	213109						

APPENDIX III

3. Cytotoxicity of CS/siRNA complexes

Table 9 (A) Cytotoxicity of chitosan hydrochloride (CS-H) in medium without serum, pH 7.2

Sample CS-H20 kDA	% cell viablility (n=3)				
N/P ratio	1	2	3	average	SD
8	120.9	96.9	106.3	**108.0**	12.1
16	115.1	117.2	92.2	**108.1**	13.9
32	111.1	110.2	100.1	**107.2**	6.1
64	113.7	116.4	122.7	**117.6**	4.6

Sample CS-H45 kDA	% cell viablility (n=3)				
N/P ratio	1	2	3	average	SD
8	112.9	104.4	108.3	**108.5**	4.2
16	96.4	103.8	103.3	**101.2**	4.1
32	103.5	87.6	98.7	**96.6**	8.2
64	102.5	104.1	115.6	**107.4**	7.1

Sample CS-H200 kDA	% cell viablility (n=3)				
N/P ratio	1	2	3	average	SD
8	111.5	93.3	114.4	**106.4**	11.4
16	114.2	120.9	119.2	**118.1**	3.5
32	110.2	111.5	113.1	**111.6**	1.4
64	103.9	108.1	116.1	**109.4**	6.2

Sample CS-H460 kDA	% cell viablility (n=3)				
N/P ratio	1	2	3	average	SD
8	115.1	120.9	121.6	**119.2**	3.5
16	101.4	107.3	114.2	**107.6**	6.4
32	118.3	109.4	108.3	**112.0**	5.5
64	113.7	103.3	100.6	**105.9**	6.9
control	103.5	99.0	97.6	**100.0**	3.1

Table 9 (B) Cytotoxicity of chitosan lactate (CS-L) in medium without serum, pH 7.2

Sample CS-L20 kDA	% cell viablility (n=3)				
N/P ratio	1	2	3	**average**	SD
8	86.0	92.7	97.9	**92.2**	6.0
16	94.3	87.7	91.3	**91.1**	3.3
32	86.5	86.0	89.9	**87.4**	2.1
64	89.4	94.9	100.2	**94.8**	5.4

Sample CS-L45 kDA	% cell viablility (n=3)				
N/P ratio	1	2	3	**average**	SD
8	95.7	77.4	97.9	**90.4**	11.3
16	91.1	82.3	76.1	**83.2**	7.6
32	105.2	79.5	75.1	**86.6**	16.3
64	85.4	94.1	78.7	**86.1**	7.7

Sample CS-L200 kDA	% cell viablility (n=3)				
N/P ratio	1	2	3	**average**	SD
8	84.8	78.4	88.0	**83.7**	4.9
16	98.7	97.9	103.4	**100.0**	3.0
32	88.0	88.3	94.6	**90.3**	3.8
64	102.5	97.4	110.0	**103.3**	6.3

Sample CS-L460 kDA	% cell viablility (n=3)				
N/P ratio	1	2	3	**average**	SD
8	88.6	98.3	92.3	**93.1**	4.9
16	93.5	97.7	94.2	**95.1**	2.3
32	84.8	100.9	102.2	**96.0**	9.7
64	91.1	109.8	103.9	**101.6**	9.6
control	103.5	99.0	97.6	**100.0**	3.1

Table 9 (C) Cytotoxicity of chitosan aspartate (CS-A) in medium without serum, pH 7.2

Sample CS-A20 kDA	% cell viablility (n=3)				
N/P ratio	1	2	3	average	SD
8	102.7	112.3	110.9	**108.6**	5.2
16	102.8	99.8	102.4	**101.7**	1.7
32	93.3	88.2	93.3	**91.6**	3.0
64	91.9	92.8	88.5	**91.1**	2.3

Sample CS-A45 kDA	% cell viablility (n=3)				
N/P ratio	1	2	3	average	SD
8	129.0	97.4	100.5	**109.0**	17.5
16	105.0	98.8	103.4	**102.4**	3.2
32	90.3	82.7	90.5	**87.8**	4.4
64	77.8	86.7	90.3	**85.0**	6.4

Sample CS-A200 kDA	% cell viablility (n=3)				
N/P ratio	1	2	3	average	SD
8	92.6	95.0	98.9	**95.5**	3.2
16	94.5	90.3	102.2	**95.7**	6.0
32	89.9	87.1	94.4	**90.5**	3.7
64	96.5	99.0	85.7	**93.7**	7.1

Sample CS-A460 kDA	% cell viablility (n=3)				
N/P ratio	1	2	3	average	SD
8	74.2	79.3	81.8	**78.4**	3.9
16	70.8	91.5	81.9	**81.4**	10.4
32	68.0	77.4	76.7	**74.0**	5.2
64	83.2	74.2	74.5	**77.3**	5.1
control	103.5	99.0	97.6	**100.0**	3.1

Table 9 (D) Cytotoxicity of chitosan glutamate (CS-G) in medium without serum, pH 7.2

Sample CS-G20 kDA	% cell viablility (n=3)				
N/P ratio	1	2	3	**average**	SD
8	97.7	93.1	88.8	**93.2**	4.5
16	104.9	84.5	80.9	**90.1**	12.9
32	101.4	85.5	80.6	**89.1**	10.9
64	83.5	81.3	92.7	**85.9**	6.1

Sample CS-G45 kDA	% cell viablility (n=3)				
N/P ratio	1	2	3	**average**	SD
8	88.9	89.8	93.2	**90.6**	2.3
16	81.3	74.2	71.6	**75.7**	5.0
32	84.3	76.3	82.8	**81.1**	4.2
64	86.4	83.8	91.7	**87.3**	4.0

Sample CS-G200 kDA	% cell viablility (n=3)				
N/P ratio	1	2	3	**average**	SD
8	77.9	72.6	82.2	**77.6**	4.8
16	72.8	73.8	82.6	**76.4**	5.4
32	71.3	81.6	88.6	**80.5**	8.7
64	88.9	75.9	80.1	**81.6**	6.6

Sample CS-G460 kDA	% cell viablility (n=3)				
N/P ratio	1	2	3	**average**	SD
8	79.0	83.3	89.2	**83.8**	5.1
16	71.3	76.0	82.4	**76.6**	5.6
32	86.6	86.0	88.6	**87.0**	1.4
64	64.7	77.7	97.4	**79.9**	16.4
control	103.5	99.0	97.6	**100.0**	3.1

BIOGRAPHY

NAME   Sirirat Wongkupasert, Miss

DATE of BIRTH   9   November 1979

PLACE OF BIRTH   Bangkok, Thailand

INSTITUTION ATTENDED

Silpakorn University, 1999 – 2003 :

Bachelor of Science (Biology)

Silpakorn University, 2006- 2008 :

Master of Pharmacy (Biopharmaceutical sciences)

PRESENTATION

1. **Sirirat Wongkupasert**, Sunee Techaarpornkul, Auayporn Apirakaramwong, Praneet Opanasopit, Jurairat Nunthanid. Characterization of lipofectamine and polyethylenimine-mediated siRNA delivery in vitro. 23th Annual meeting of the faculty of pharmaceutical sciences Chulalongkorn University and JSPS 1st Medicinal chemistry seminar of asia/africa scientific program December 14-15, 2006; Bangkok, Thailand.

2. Praneet Opanasopit, **Sirirat Wongkupasert**, Sunee Techaarpornkul, Auayporn Apirakaramwong, Jurairat Nunthanid. Chitosan-Mediated siRAN Delivery in Vitro: Effect of Polymer Molecular Weight and Salt Forms. 34th Annual meeting of the controlled release society July 7-11, 2007; Long Beach Convention Center, Long Beach, California, USA.

3. **Sirirat Wongkupasert**, Sunee Techaarpornkul, Praneet Opanasopit, Auayporn Apirakaramwong, Jurairat Nunthanid and Uracha Ruktanonchai

"Chitosan lactate as siRNA delivery in stable and constitutive EGFP-expressing cells" Proceedings of the 5th Pharma-Indochina conference in Pharmacy for sustainable development, November 21-24, 2007 Bangkok, Thailand.

4. Praneet Opanasopit, Sunee Techaarpornkul, **Sirirat Wongkupasert**, Auayporn Apirakaramwong, Jurairat Nunthanid and Mitsuru Hashida. Galactosylated chitosan for siRNA delivery in stable constitutive eGFP-HepG2 cells. 3rd Asian association of Schools of pharmacy (AASP) conference October 25th-28th 2007 at the Renaissance Makati City Hotel, Makati City, Philippines.